NASA TN D-167

NASA TN D-167

7N-02
197228
47P

TECHNICAL NOTE

D-167

INVESTIGATION OF VARIATION IN BASE PRESSURE OVER THE REYNOLDS NUMBER RANGE IN WHICH WAKE TRANSITION OCCURS FOR TWO-DIMENSIONAL BODIES AT MACH NUMBERS FROM 1.95 TO 2.92

By Vernon Van Hise

Langley Research Center
Langley Field, Va.

NATIONAL AERONAUTICS AND SPACE ADMINISTRATION

WASHINGTON November 1959

1B

NATIONAL AERONAUTICS AND SPACE ADMINISTRATION

TECHNICAL NOTE D-167

INVESTIGATION OF VARIATION IN BASE PRESSURE OVER THE REYNOLDS NUMBER RANGE IN WHICH WAKE TRANSITION OCCURS FOR TWO-DIMENSIONAL BODIES AT MACH NUMBERS FROM 1.95 TO 2.92

By Vernon Van Hise

L
5
1
5

SUMMARY

An investigation has been made to determine the effect of Reynolds number upon two-dimensional base pressure throughout the Reynolds number range of wake transition. Base-pressure variation with Reynolds number was found to agree qualitatively with the theoretical predictions of Crocco and Lees throughout wake transition. Fineness-ratio effects upon base pressure were relatively large and agreed qualitatively with theory. Model-shape effects upon base pressure became significant for fineness ratios of about 3 but were negligible for fineness ratios of about 8. The wake-minimum-disturbance length varied greatly with Reynolds number. The point of convergence of the shocks originating downstream of the wake dead-air region was found to be a good indication of the minimum-disturbance length. The tests covered a Reynolds number range of approximately 5,000 to 6,000,000 and a Mach number range of 1.95 to 2.92.

INTRODUCTION

The problem of predicting two-dimensional base pressure is one of prime importance at moderate supersonic speeds in that base pressure can produce a large portion of the total drag. Indeed, the problem has gained much interest with the advent of the blunt-trailing-edge concept. The available experimental data of two-dimensional base pressure for the Reynolds number range of wake transition is rather limited to date. About the most extensive investigation for the realm of wake transition has been given in reference 1. The data of that investigation cover the middle Reynolds number range of wake transition, the complete realm of wake transition being considered as covering the Reynolds number range over which the critical wake region first contains turbulent flow until it becomes completely turbulent.

Two different analyses of the base-pressure problem have been made. The first is the mixing theory of Crocco and Lees (ref. 2) which utilizes the momentum-integral method of boundary-layer theory and considers mixing between the outer, nearly isentropic stream and the dissipative wake region as the fundamental process for determining base pressure. The second analysis is presented in references 3 and 4 in which the dynamics of the streamline which bounds the circulatory portion of the wake is formulated to evaluate base pressure. One of the more interesting predictions of the theory of Crocco and Lees is the occurrence of a maximum in base pressure at a Reynolds number of approximately 50,000. This same maximum was examined in reference 5 in which the analysis of reference 4 was modified to justify its occurrence.

The purpose of this paper is to present the results of a wind-tunnel study of two-dimensional base pressure throughout the realm of wake transition. Some factors to be examined which affect base pressure are model shape and model fineness ratio. Also included in the tests was a wake-disturbance study along with some schlieren studies. Tests were conducted at Mach numbers from 1.95 to 2.92 and over a Reynolds number range of approximately 5,000 to 6,000,000.

SYMBOLS

b	model span
c	model chord length
$C_{p,b}$	base-pressure coefficient referred to free-stream conditions, $\frac{p_b - p}{q}$
d	disturbance-probe height
F	model fineness ratio, $\frac{c}{h}$
h	model-base height
l	minimum disturbance length, measured rearward from model base in chordwise direction
M	free-stream Mach number
M_{nom}	nominal test-section Mach number
p	free-stream static pressure

p_b base pressure

p_s surface pressure

p_t stagnation pressure in stagnation chamber

p_t' free-stream stagnation pressure

q free-stream dynamic pressure, $\frac{\gamma}{2} pM^2$

L515

r chordwise distance from model base to convergence point of wake trailing shock system (see fig. 1)

R free-stream Reynolds number based on model chord length

x chordwise distance from model nose

γ ratio of specific heats for air, 1.4

δ model wedge half angle

APPARATUS

Wind Tunnel and Auxiliary Equipment

The Langley 9-inch supersonic tunnel is a continuous-operation, closed-circuit type in which the pressure, temperature, and humidity of the enclosed air can be regulated. Different test Mach numbers are provided by interchangeable nozzles which form test sections approximately 9 inches square. Eleven fine-mesh turbulence-damping screens are installed in the relatively large-area settling chamber ahead of the supersonic nozzle. The turbulence level of the tunnel, based on the turbulence-level measurements presented in reference 6, is considered low. A schlieren optical system is provided for qualitative flow observations.

The free-stream static pressure p, the model-surface pressure p_s, and the base pressure p_b were measured with liquid butyl phthalate manometers. These manometers are referred to a vacuum and have a pressure range from 0 to 130 millimeters of mercury absolute. All other test pressures were measured with a mercury manometer.

Models

Figure 2 presents drawings of the base-pressure test models along with a series of disturbance probes. The main variables for the base-pressure models of figures 2(a), 2(b), and 2(c) are summarized in table I. Model 11 was also used to obtain surface pressure distributions. This model was constructed after model 2 had been tested by adding a straight detachable afterbody to model 2. Model 11 had surface orifices located at chordwise stations so that, by testing with and without the straight afterbody, the upstream influence upon surface pressure of the expansion at the base of model 2 could be ascertained. Figure 2(d) shows the series of disturbance probes (nos. 1, 2, and 3) which were translated fore and aft in the wakes of models 2 and 3 to find minimum disturbance lengths l above which base pressure is unaffected.

L
5
1
5

All test models were supported between the tunnel sidewalls which are $8\frac{3}{4}$ inches apart. The larger models spanned the width of the tunnel test section whereas the smaller models were supported in the center of the tunnel test section by supports which protruded from the sidewalls. Models 2 and 3 had spans of $b = 18$ inches so that a spanwise base-pressure distribution could be obtained by sliding these models through the tunnel sidewalls. Models 1, 2, 3, 4, and 6 have their base-pressure orifices distributed about the base to obtain base-pressure distributions in the spanwise and vertical directions on the base. Boundary-layer end plates were included in the tests of models 1, 2, and 6 to ascertain tunnel boundary-layer effects upon base pressure. All test model pressures were transmitted to the butyl phthalate manometers by tubing which was embedded in a spanwise fashion along the model and its support system and thus through the tunnel walls to the manometers.

The models were constructed of stainless steel. Their leading-edge thicknesses were considered to have negligible effect upon model pressures. The initial finish of the model surfaces was obtained by standard machining and polishing procedures, and a more highly finished surface was obtained by polishing with metal polish and fine polishing stone. (Similar polishing has been found to give a root-mean-square surface roughness of about 8 microinches.) Before testing, the models were checked for surface smoothness and wiped clean of foreign matter and fingerprints. These efforts to make the model as polished and clean as possible are essential in obtaining consistent base-pressure data inasmuch as transition, the location of which determines base pressure, is known to be very sensitive to model surface conditions.

TESTS

For this investigation the wind tunnel was operated at stagnation pressures which varied from 5 inches of mercury absolute to 3.5 atmospheres absolute with stagnation temperatures between 65° F and 120° F. Schlieren observations of the flow pattern were made to determine whether any disturbances were affecting the region of the model wakes. The models were maintained as closely as possible at a condition of zero pitch and zero yaw.

Tests were conducted at the nominal test-section Mach numbers of 1.95, 2.22, 2.62, and 2.92. At Mach numbers of 1.95 and 2.62, the tests were mainly concerned with base-pressure variation with Reynolds number for a given body shape. At Mach numbers of 2.22 and 2.92, more extensive testing was done and the additional items of model fineness ratio and model shape were considered for their effects upon base pressure. Also considered at these two Mach numbers were Reynolds number effects upon surface pressure distribution in conjunction with determining the upstream influence of base-pressure phenomena upon surface pressure. At a Mach number of 2.92, an extensive examination of the wake region was made by means of pressure measurements and schlieren observations. (See fig. 1 for test setup.)

During each test the independent parameter, Reynolds number, was varied by regulating the tunnel stagnation pressure, and base-pressure data were taken for each model from the minimum up to the maximum attainable stagnation pressure. This procedure gave base-pressure readings within various Reynolds number ranges, depending on model chord length, with enough overlapping of Reynolds number for the various models so that scale effects could be ascertained. The overall Reynolds number range of approximately 5,000 to 6,000,000 gave base-pressure data throughout most, if not all, of the Reynolds number range for which wake transition occurs.

Past investigations in supersonic wind tunnels have shown that the scale of the flow (Reynolds number per unit length) may have a significant effect upon the Reynolds number at which transition moves onto a body. For the wind tunnel used in the present tests, several previous investigations (see ref. 7, for example) indicate that this transition Reynolds number increases with increasing stagnation pressure by a factor of about 2 for the range of stagnation pressures of this investigation. No attempt is made in this investigation to evaluate the effect that scale of the flow might have upon wake transition and, therefore, upon base pressure; however, some effect would be expected.

INTERPRETATION AND REDUCTION OF DATA

Tunnel Mach Number Variation

Throughout the stagnation-pressure range of the present tests, significant variation in test-section Mach number occurred. Both a static-pressure survey and pitot-tube survey were obtained at that position along the center line of the wind tunnel where the model bases were located. By using the survey data, the test-section Mach number and the stagnation-presssure loss occurring between the stagnation chamber and the test section were calculated as a function of stagnation-chamber pressure. Curves of these variations are shown in figures 3 and 4 for the various nominal test-section Mach numbers.

L515

It is seen that test-section flow conditions vary rapidly below a stagnation pressure of about 1/2 atmosphere absolute. Possible factors contributing to this rapid variation in test-section Mach number and stagnation-pressure loss are variations in the thickness of the boundary layer on the wind-tunnel walls, water-vapor condensation in the airstream, and low-pressure errors in the pressure measurements themselves. (Ref. 8 presents comparable variations in test-section flow conditions due to these factors.) All values of Reynolds number and base-pressure coefficient have been computed for the measured test conditions determined by these surveys.

Interference Considerations

Inasmuch as the spans of the larger models were limited by the width of the tunnel, consideration was given to tunnel boundary-layer disturbances feeding into the critical-wake region (the region extending the distance l behind the model base). It should be noted here that, with or without end plates, spanwise base-pressure distributions indicated that the base pressure was two dimensional over at least the central portion of the model span. Boundary-layer end plates used in the tests of models 1, 2, and 6 showed that base pressures were disturbance free except for model 1 at Mach numbers 2.62 and 2.92, model 1 having the largest base height of all the models tested. Disturbance free means that the base pressure was essentially the same with or without end plates. For model 1 without end plates, visible manometer oscillations of base pressure were observed; these oscillations were relatively slight at Mach number 2.62 but were severe at Mach number 2.92. The average base-pressure reading obtained with slight oscillations agreed with the readings obtained with end plates whereas readings obtained with severe oscillations were found to contain considerable disturbance error. Except for model 5, the rest of the models were of much smaller size than those checked with end plates and are considered to give interference-free two-dimensional base-pressure data. Model 5 was constructed during the test program and had no end plates. However, the base-pressure readings of model 5 were observed to be free of violent oscillation due to tunnel boundary-layer disturbance, although at Mach number 2.92 slight oscillation, heretofore considered insignificant, was found. All base-pressure data presented have been judged as two dimensional and disturbance free in accordance with the previous discussion.

The disturbance probes had spans about 1/3 of the base-pressure-model span in the wake-study tests. Spanwise base-pressure measurements showed that the wake flow over almost the complete probe span was two dimensional when minimum disturbance lengths were being measured. Hence, the disturbance-probe tests were judged as giving two-dimensional data.

Precision of Data

All models were maintained within $\pm 0.25^{\circ}$ of zero pitch and yaw. Past measurements of the flow angularity in the tunnel test section have shown negligible deviations. All pressure measurements were read within ±0.01 inch of the given manometer fluid, either mercury or butyl phthalate. The estimated overall accuracies of the main test variables are as follows:

Mach number, M (at 1 atmosphere stagnation pressure)	± 0.01
Reynolds number, R $\left(\text{probable error at } R = 1 \times 10^{6}\right)$	$\pm 0.01 \times 10^{6}$
Base-pressure coefficient, $C_{p,b}$	± 0.002

RESULTS AND DISCUSSION

Basic Data

Figure 5 is a compilation of all base-pressure-coefficient data obtained in this investigation. Base-pressure coefficient is presented as a function of Reynolds number for the various nominal Mach numbers and model shapes. Each data point is based on the true Mach number corresponding to the particular stagnation pressure; hence, the data points give base-pressure-coefficient curves along which the Mach number varies. However, the curves would be negligibly affected by this Mach number change except at the lower Reynolds number for each curve where Mach number decreases rapidly as the Reynolds number is decreased.

The data of figure 5 are for an angle of attack of 0°. However, tests at an angle of attack of 7° indicated no change in base pressure. Also, it was found that along the height of the base there was no variation in base pressure for angles of attack of either 0° or 7° throughout the Reynolds number and Mach number variation of the tests. This is as concluded in reference 1, in which it was ascertained that the two-dimensional supersonic wake is isobaric upstream of the wake recompression region.

Analysis of Models 1 to 8

The discussion to follow is concerned with transforming the basic data of figure 5 into a form more suitable for analysis. Figure 6 shows the base-pressure-coefficient data for models 1 to 8. The curves are tracings of the faired curves of figure 5, only grouped now with respect to model shape. Figure 6(a) presents models 1 to 4 which are all ogives with a fineness ratio of 3. Figure 6(b) presents models 5 to 8 which have a fineness ratio of 8 but which have different shaped cross sections (wedge and ogival) as shown in figure 2(b). All the curves of figure 6 still contain varying Mach number effects; however, it might be suspected that scale effects are small enough to be neglected in the overall picture. Figure 6(b) indicates an expected trend, namely that shape loses its importance in affecting base pressure when the fineness ratio becomes large enough that free-stream Mach number and static pressure are attained before the expansion about the base. Hence, models 5 to 8 are referred to only by their fineness ratio of 8.

Figure 7 presents base-pressure-coefficient data in cross-plotted form with base-pressure coefficient as a function of Mach number at various constant Reynolds numbers. These cross plots were obtained from the curves of figure 6. By cross plotting in this fashion tunnel Mach number variations no longer present a problem. For instance figure 7(a) with $R = 250,000$ shows vividly how the difference in base-pressure coefficient for different models at the same Reynolds number, obtained in the original data, is largely due to tunnel Mach number variation. The curves of figure 7(a) have deviations in base-pressure-coefficient points of about ± 0.004 from the faired curves while those of figure 7(b) have deviations of about ± 0.006. These deviations are greater than the maximum probable error in measured base-pressure coefficient and can be attributed for the most part to scale effects and, in the case of figure 7(b), also to model shape. However, the deviations are relatively slight so that scale and model shape effects can be neglected in the analysis of models 1 to 8.

From the constant Reynolds number curves of figure 7, final plots of base-pressure variation were constructed. These are shown in figure 8 in which base-pressure coefficient is plotted as a function of Reynolds number with the values of the nominal test-section Mach numbers as parameters. It can be seen from this figure that as the degree of turbulence in the wake lessens (proceeding from high to low Reynolds number) the degree of variation of base-pressure coefficient with Mach number also lessens. This is as occurred for the case of the body of revolution with a fineness ratio of 8 (ref. 9); in fact, the base-pressure coefficient was almost invariant with Mach number in the Reynolds number region of about 50,000 (the region in which the critical wake region is almost completely laminar). Critical wake region refers to that portion of the wake extending rearward from the base to the station downstream of which disturbances do not affect base pressure. (This is in accordance with the theory of Crocco and Lees in ref. 2.) These curves of figure 8 give a Reynolds number coverage of wake transition as the critical wake region progresses from an almost, if not entirely, laminar flow to a completely turbulent flow at Mach numbers from 1.95 to 2.92.

Figures 9 and 10 present the curves of figure 8 in combined form so that fineness-ratio effects upon base-pressure coefficient and base-pressure ratio p_b/p can be ascertained. Consider the base-pressure ratio curves of figure 10 for Reynolds numbers of wake transition, that is, for Reynolds numbers less than the Reynolds number of minimum base pressure. It is seen that increasing the fineness ratio for a given Reynolds number and Mach number increases base pressure. Since model-shape effects are comparatively small, most of this increase in base pressure can be attributed to a decrease in base height. When transition is located within the critical wake region, a decrease in base height causes a greater portion of this region to become laminar; hence, base pressure increases with increasing fineness ratio (theory of Crocco and Lees).

According to the theory of Crocco and Lees, the decrease in base pressure with decreasing Reynolds number for the region to the left of the base-pressure maximums (fig. 10) is due to an increasing laminar mixing rate. This concept makes it possible for base pressure to decrease with increasing fineness ratio for low Reynolds numbers. Figure 10 indicates that the $F = 8$ curves may fall below the $F = 3$ curves at some Reynolds number below 20,000.

Figure 11 gives a comparison of the base-pressure variation with Reynolds number for two-dimensional flow (present investigation) as opposed to axisymmetric flow (ref. 9) for the conditions of identical Mach number, fineness ratio, and wind tunnel. The axisymmetric flow gives a higher level of base pressure which is understandable since there is a relieving effect in three-dimensional flow which makes expansions and shocks less severe than for the two-dimensional case.

The theory of Crocco and Lees evidently gives a qualitative explanation of what occurs in both the axisymmetric- and two-dimensional-base problems although it was derived only for the two-dimensional problem.

Some main predictions of this theory were that a maximum in base pressure existed when the critical-wake region was almost completely laminar and that a minimum in base pressure existed when the critical wake region became completely turbulent, both predictions being exemplified in figures 10 and 11. An analysis of the supersonic wake in the Reynolds number region of maximum base pressure is given in reference 5 in which the theory of reference 4 was modified and the concept of a maximum in the two-dimensional base-pressure curve was justified. During the present investigation shadowgraphs at low Reynolds numbers (around 20,000) indicated a shortening of the dead-air region behind the base as Reynolds number decreased; this shortening corresponds to the measured decrease in base pressure.

L
5
1
5

Some Additional Shape Comparisons

Figure 12 presents the base-pressure data of model 11 ($F = 6$) in addition to portions of the curves of figure 10 ($F = 3$ (ogives) and $F = 8$) for the Mach numbers 2.22 and 2.92. It must be remembered that $F = 6$ curves have a slightly varying Mach number. However, the basic trends are still in agreement with previous discussion when it was considered plausible that base pressure should increase with fineness ratio for a given Reynolds number and Mach number.

Figure 13 is a reproduction of the basic data of models 9 and 10 given in figure 5 at the nominal Mach numbers 2.22 and 2.92. The fairing of the curves has been done with due regard to slightly varying Mach numbers and scale effects, and is considered to give a fairly accurate representation of the base-pressure variation for this model shape ($F = 3$; wedge, $\delta = 30^\circ$). Figure 14 shows these curves in the form of base-pressure ratio p_b/p and compares them with the curves of corresponding Mach number from figure 10. Probably the most interesting comparison to make is between the ogive and wedge shapes with fineness ratio 3. Going from an ogive with nose half angle about 20° to a wedge with $\delta = 30^\circ$ has raised the maximum base pressure and shifted it to a lower Reynolds number. These effects are attributed to the change in flow conditions just before the base expansion; changing from the ogive to this wedge shape has caused a stronger nose shock (indeed the shock is detached from the wedge at Mach number 2.22) so that conditions just before the base are even further removed from free-stream values. Thus if base pressure is based on free-stream Mach number and Reynolds number as it is in figure 14, body shape can significantly affect base pressure for fineness ratios on the order of 3 for Mach numbers of about 3.

Surface Pressure Distribution

The determination of how far upstream from the base the expansion towards base pressure begins is depicted in figure 15 for a Reynolds number of 300,000 at Mach numbers 2.22 and 2.92. Data were obtained for Reynolds numbers as low as 100,000 but it was found to be essentially the same as that for 300,000. For these Reynolds numbers and Mach numbers the base-pressure ratio p_b/p is always about 0.5 and hence it may be stated that effects of the base-pressure phenomena upon surface pressure become more prominent as Mach number is decreased for the present range of variables. It is noted, for instance, that for the last surface pressure station in the ogive alone case the flow has expanded toward the base pressure more completely at Mach number 2.22 as compared to 2.92. In any case, figure 15 shows that base-pressure effects upon surface pressure can become significant in determining correct overall model forces especially for small fineness ratios.

L
5
1
5

Wake Region Analysis

According to the theory of Crocco and Lees a singularity occurs in the basic differential equation which they have derived to govern two-dimensional supersonic wake flow. This singularity indicates that a critical point exists at some point downstream of the base with the characteristic that disturbances introduced into the wake at positions downstream of this critical point are not able to affect the base pressure. The region between the base and the critical point is referred to as the critical wake region. In order to determine Reynolds number effects upon the extent of this critical wake region, a series of disturbance-probe tests were made to obtain the minimum disturbance length l. Tests were made for the ogive shape with a fineness ratio of 3 at the nominal Mach number of 2.92.

Figure 16 presents the variation of l/h with Reynolds number and contains data obtained with various combinations of the available model and probe sizes. It should be noted that these data were obtained by moving the probes toward the bases in approximately $h/2$ increments, and the value l was considered reached for that increment previous to the increment for which a greater than 1-percent variation in base pressure first occurred. By considering only the solid-line data at present, the model and probe combination was found to give an array of data through which two distinct lines could be faired. The lines are distinguished by the parameter d/h, the ratio of probe height to base height. The reason for this effect of d/h is readily observed in the schlieren photographs of figure 16. (The probes have been outlined and cross hatched with white ink.) For small values of d/h (fig. 17(a)) it is seen that, when relative scale size is considered, the probe tip has essentially an attached shock. However, for large values of d/h (fig. 17(b)) the probe-nose shock has been displaced forward on the order of 1 base height. Hence, the larger d/h probe will have a larger minimum disturbance length when distances are based on the position of the probe nose tip itself.

Figure 16 indicates a marked variation of l/h with Reynolds number. Even though a maximum in base pressure has occurred at a Reynolds number of about 100,000 (see curve in fig. 10 for $F = 3$, $M = 2.92$), l/h is still increasing with decreasing Reynolds number below 100,000. In reference 10, this same variation was found to occur for bodies of revolution. It was theorized (ref. 10) that, as Reynolds number is decreased, a maximum value of l would occur when the critical wake region becomes completely laminar (transition starts to move downstream of the critical point). This concept gives logic to why l/h is still increasing with decreasing Reynolds number even though a maximum in base pressure has already occurred, since the theory of Crocco and Lees indicates that the critical wake region contains a portion of turbulent flow at the point of maximum base pressure.

Figure 18 presents a group of wake-study schlieren photographs. Model 4 was wire supported during the visual tests, since this made the complete model visible through the test-section windows (the wire support is visible in front of the model which has been sketched with white ink). An examination of the wake trailing shock system showed that the distance behind the base of the shock system's point of convergence (this distance denoted as r) was very nearly equal to l. The position of r/h for several Reynolds numbers is shown in figure 18. A guide line has been drawn in ink parallel to the portion of trailing shock downstream of r so that it may be seen more easily how r, taken to be the point at which the trailing shock has become essentially straight, has been located. These values of r form the dashed curve of figure 16. Inasmuch as this curve agrees well with the l/h curves of the disturbance probe tests, it might be concluded that at a Reynolds number of 20,000 the minimum disturbance length is still increasing with decreasing Reynolds number. That r is a good indication of the value of l is not just peculiar to a Mach number of 2.92. A check of the schlieren photographs in reference 11 found this to be true at Mach number 2.41 for Reynolds numbers of 50,000 and greater.

CONCLUSIONS

An investigation has been made to determine the effects of Reynolds number upon two-dimensional base pressure throughout the realm of wake transition. The Mach number varied from 1.95 to 2.92 and the Reynolds number range was approximately 5,000 to 6,000,000 based on body chord length. The following conclusions were established:

1. The variation of base pressure with Reynolds number agreed qualitatively with the theoretical predictions of Crocco and Lees. In particular, the Reynolds number range investigated carried the base pressure from a maximum which corresponds to an almost completely laminar critical wake region to a minimum which corresponds to a completely turbulent critical wake region.

L
5
1
5

2. Fineness-ratio effects upon base pressure agreed qualitatively with theory.

3. Model shape effects upon base pressure became significant for fineness ratios of about 3 but were negligible for fineness ratios of about 8.

4. The wake-disturbance studies showed that minimum disturbance length varied greatly with Reynolds number and contained the same characteristics as occurred for bodies of revolution.

5. The point of convergence of the shocks originating downstream of the wake dead-air region was found to be a good indication of the minimum disturbance length.

Langley Research Center,
National Aeronautics and Space Administration,
Langley Field, Va., August 21, 1959.

REFERENCES

1. Charwat, A. F., and Yakura, J. K.: An Investigation of Two-Dimensional Supersonic Base Pressures. Jour. Aero. Sci., vol. 25, no. 2, Feb. 1958, pp. 122-128.

2. Crocco, Luigi, and Lees, Lester: A Mixing Theory for the Interaction Between Dissipative Flows and Nearly Isentropic Streams. Jour. Aero. Sci., vol. 19, no. 10, Oct. 1952, pp. 649-676.

3. Korst, H. H., Page, R. H., and Childs, M. E.: A Theory for Base Pressure in Transonic and Supersonic Flow. ME Tech. Note 392-2 (Contract No. AF 18(600)-392), Univ. of Illinois, Eng. Exp. Station, Mar. 1955.

4. Chapman, Dean R., Kuehn, Donald M., and Larson, Howard K.: Investigation of Separated Flows in Supersonic and Subsonic Streams With Emphasis on the Effect of Transition. NACA TN 3869, 1957.

5. Charwat, A. F.: A Modified Model of the Supersonic Laminar Wake. Jour. Aero/Space Sci. (Readers' Forum), vol. 25, no. 12, Dec. 1958, pp. 796-797.

6. Love, Eugene S., Coletti, Donald E., and Bromm, August F., Jr.: Investigation of the Variation With Reynolds Number of the Base, Wave, and Skin-Friction Drag of a Parabolic Body of Revolution (NACA RM-10) at Mach Numbers of 1.62, 1.93, and 2.41 in the Langley 9-Inch Supersonic Tunnel. NACA RM L52H21, 1952.

7. Grigsby, Carl E., and Ogburn, Edmund L.: Investigation of Reynolds Number Effects for a Series of Cone-Cylinder Bodies at Mach Numbers of 1.62, 1.93, and 2.41. NACA RM L53H21, 1953.

8. Hill, J. A. F., Baron, J. R., Schindel, L. H., Markham, J. R.: Mach Number Measurements in High-Speed Wind Tunnels. AGARDograph 22, North Atlantic Treaty Organization (Paris), Oct. 1956.

9. Van Hise, Vernon: Investigation of Variation in Base Pressure Over the Reynolds Number Range in Which Wake Transition Occurs for Nonlifting Bodies of Revolution at Mach Numbers from 1.62 to 2.62. NACA TN 3942, 1957.

10. Kavanau, L. L.: Base Pressure Studies in Rarefied Supersonic Flows. Jour. Aero. Sci., vol. 23, no. 3, Mar. 1956, pp. 193-207.

11. Love, Eugene S.: Base Pressure at Supersonic Speeds on Two-Dimensional Airfoils and on Bodies of Revolution With and Without Fins Having Turbulent Boundary Layers. NACA TN 3819, 1957. (Supersedes NACA RM L53C02.)

L
5
1
5

TABLE I

DESCRIPTION OF BASE-PRESSURE MODELS

Model number	Figure	Cross section	Fineness ratio, F	Chord length, c, in.	Wedge half-angle, δ, deg
1	2(a)	Ogive	3	3.6	
2	2(a)	Ogive	3	1.0	
3	2(a)	Ogive	3	.300	
4	2(a)	Ogive	3	.150	
5	2(b)	Wedge	8	6.0	10
6	2(b)	Ogive	8	2.5	
7	2(b)	Wedge	8	.50	20
8	2(b)	Wedge	8	.25	20
9	2(c)	Wedge	3	.30	30
10	2(c)	Wedge	3	.051	30
11	2(c)	Ogive plus straight section	6	2.0	

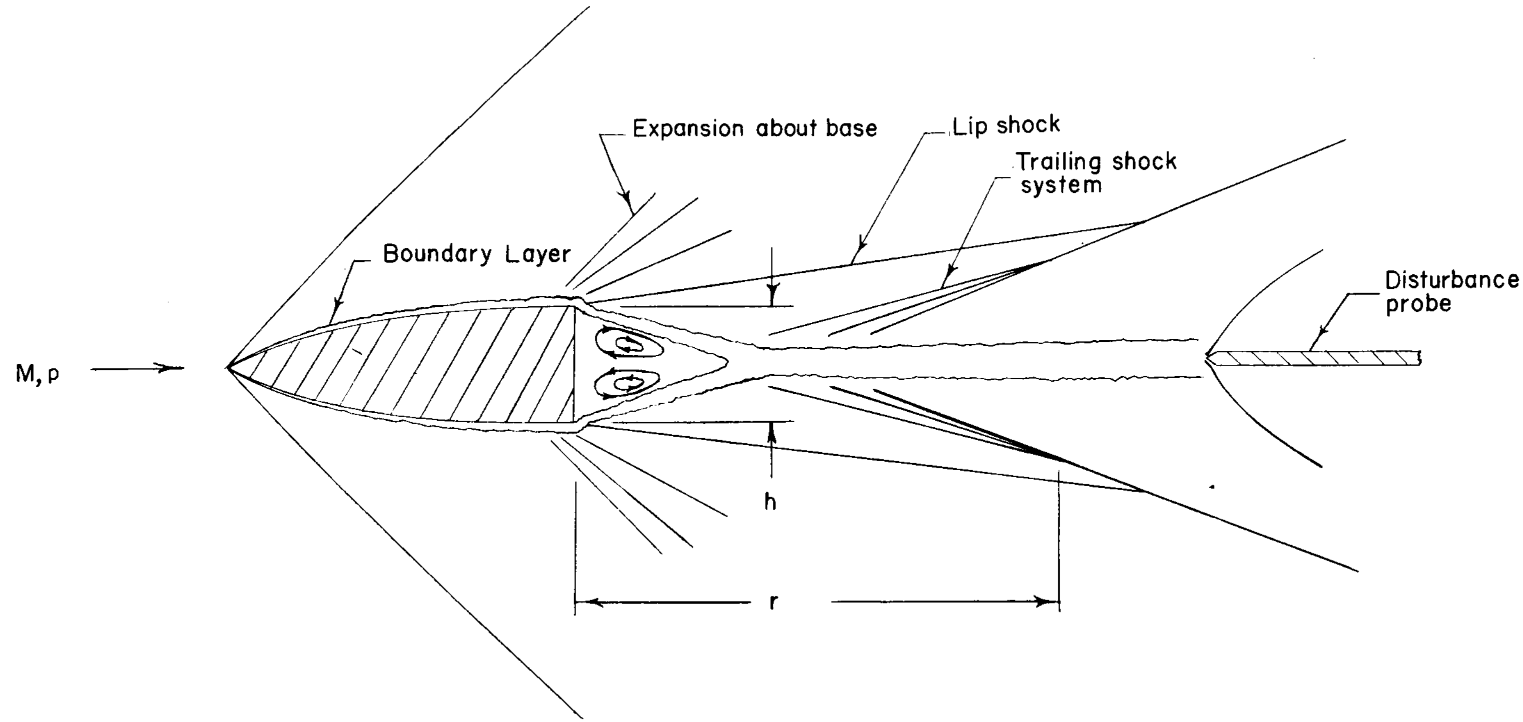

Figure 1.- Schematic representation of flow for typical test case.

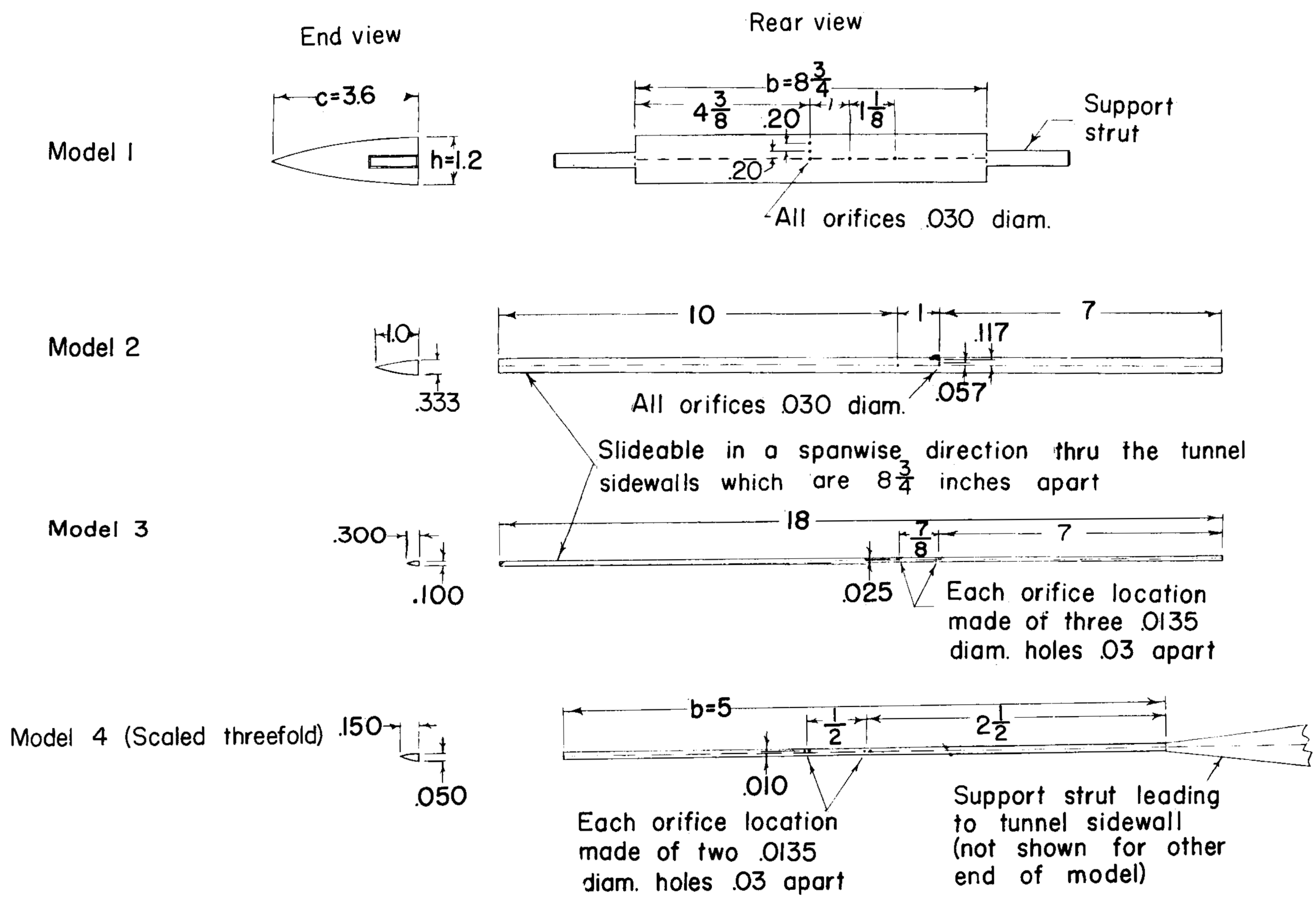

(a) F = 3, ogival series of models.

Figure 2.- Drawings of test models and disturbance probes. All linear dimensions in inches.

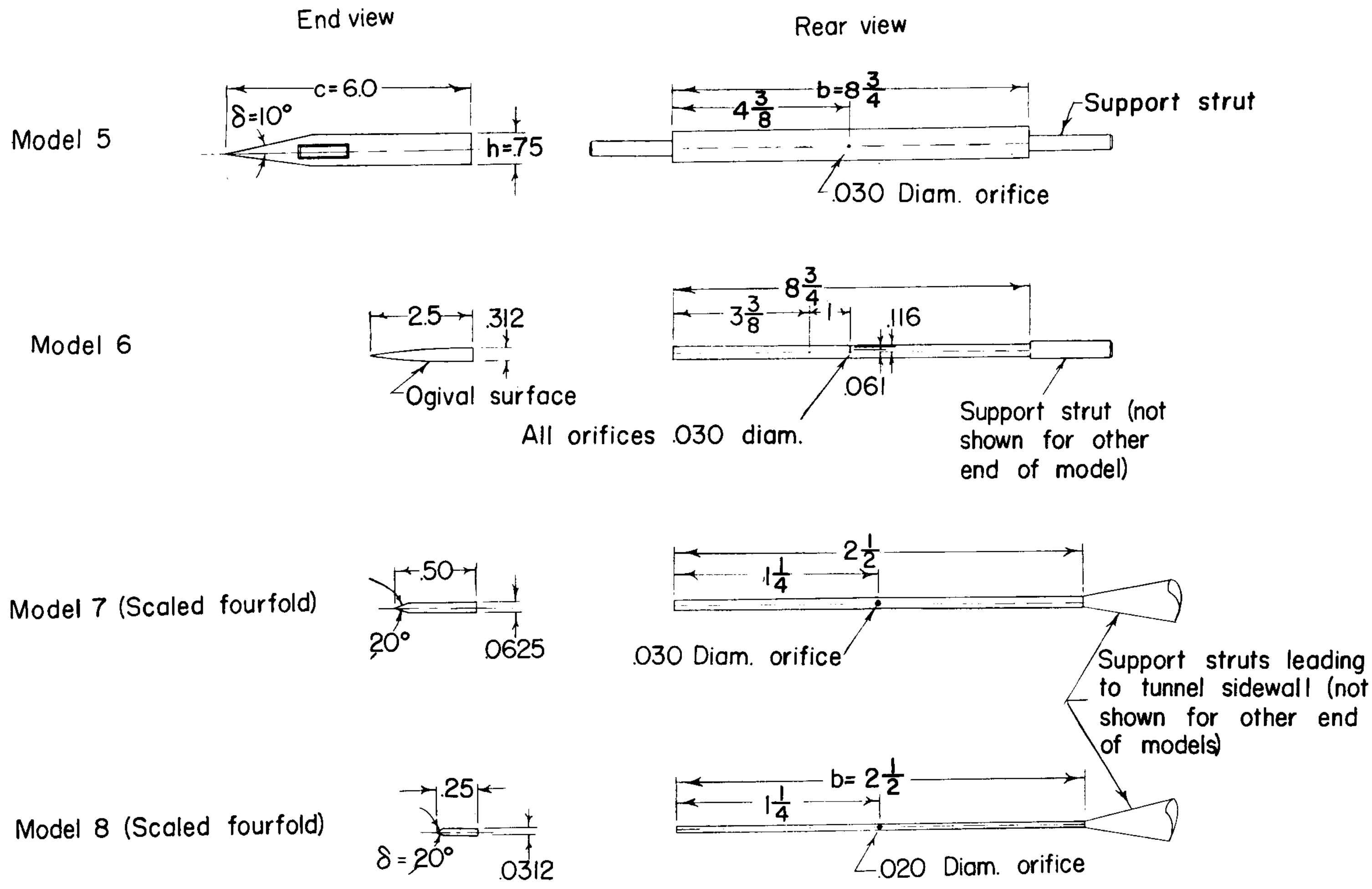

(b) F = 8, assorted shaped series of models.

Figure 2.- Continued.

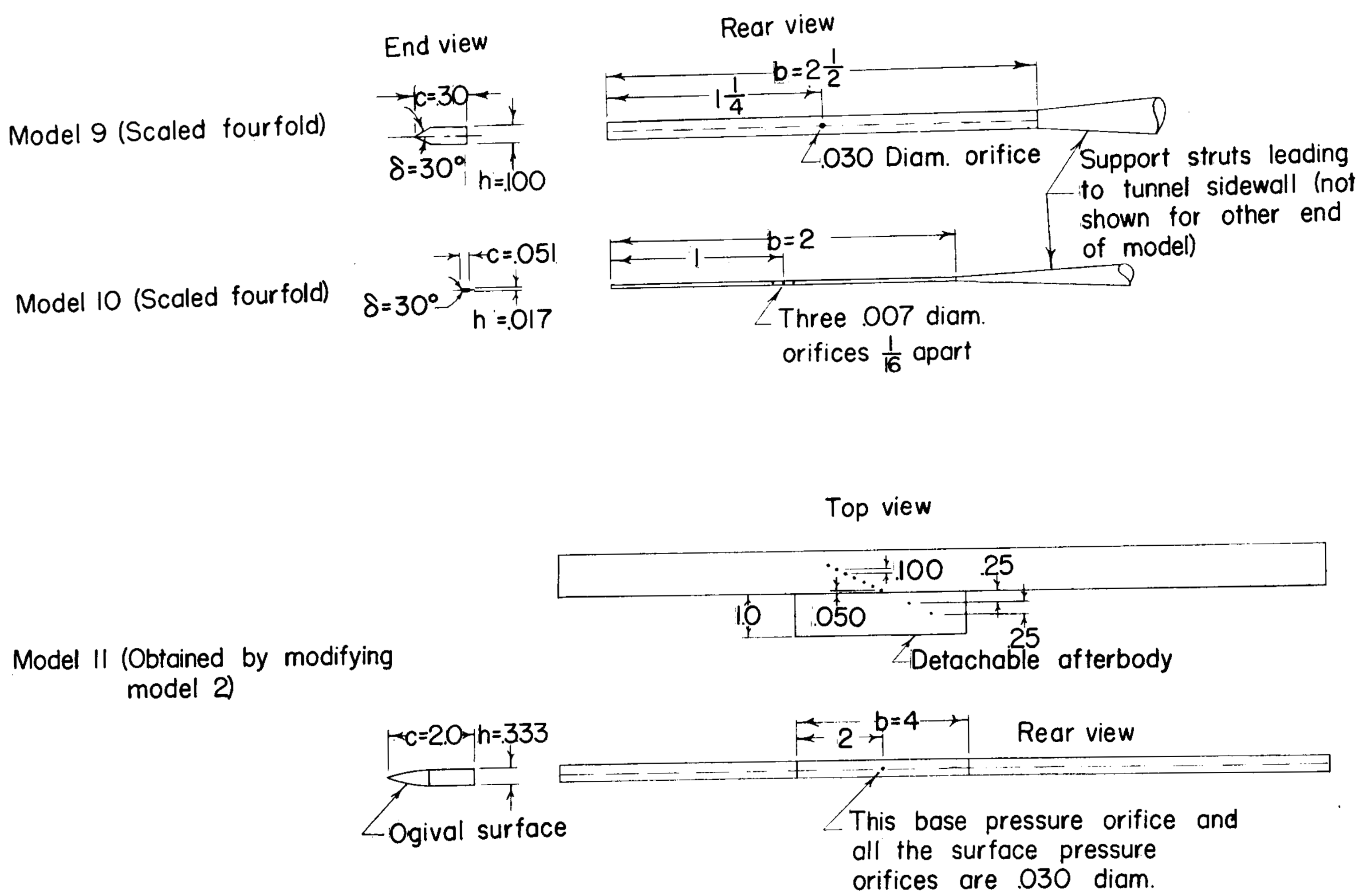

(c) Wedge-shaped models (F = 3) and surface-pressure model.

Figure 2.- Continued.

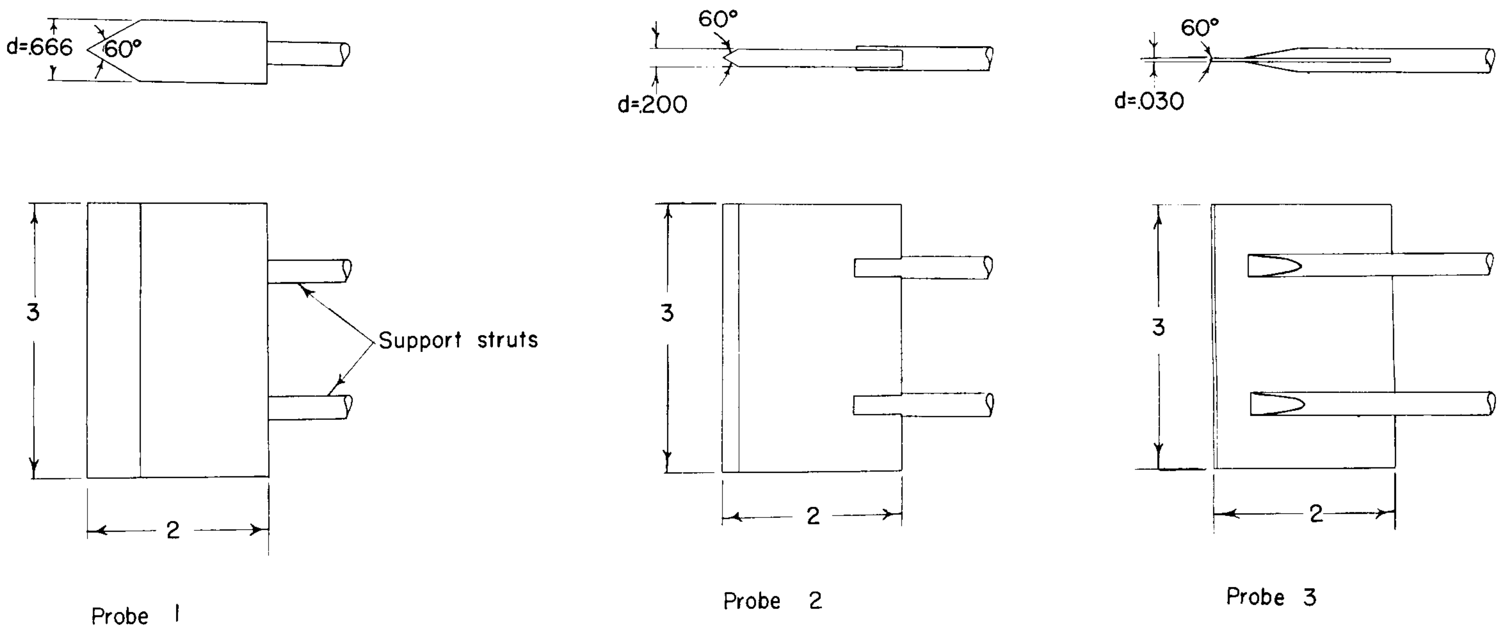

(d) Series of disturbance probes.

Figure 2.- Concluded.

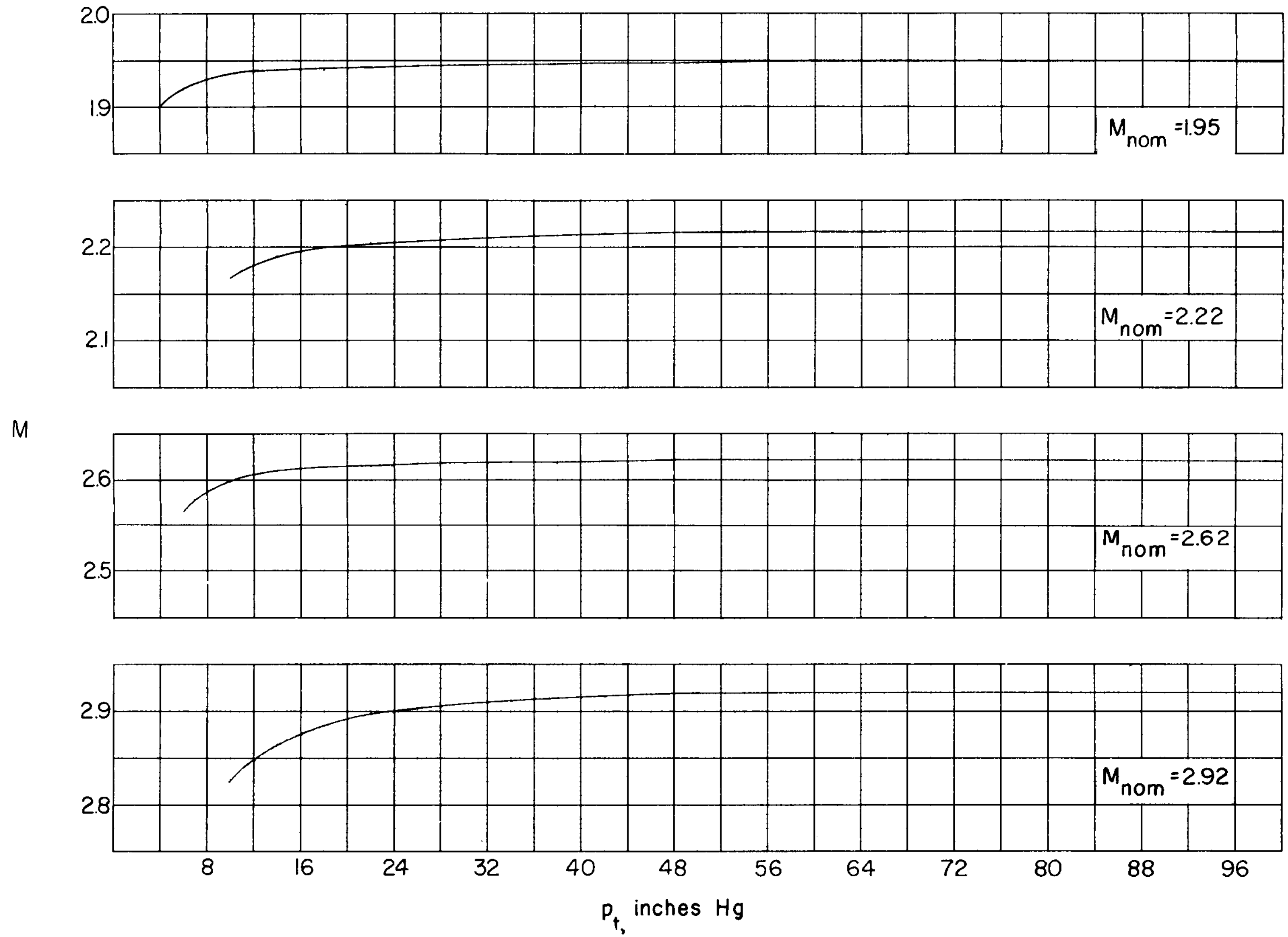

Figure 3.- Effect of tunnel stagnation-chamber pressure upon Mach number.

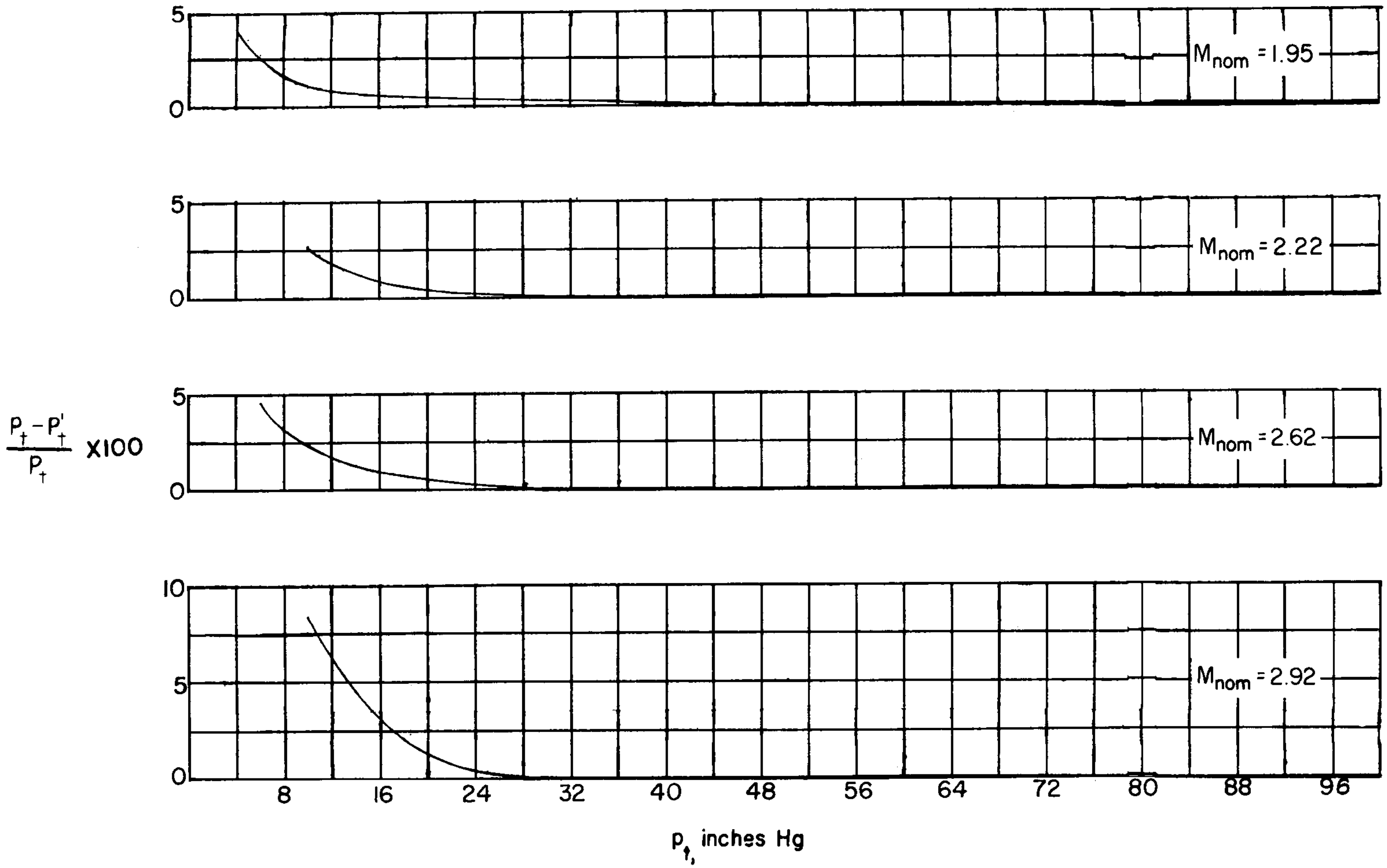

Figure 4.- Percent loss of stagnation-chamber pressure.

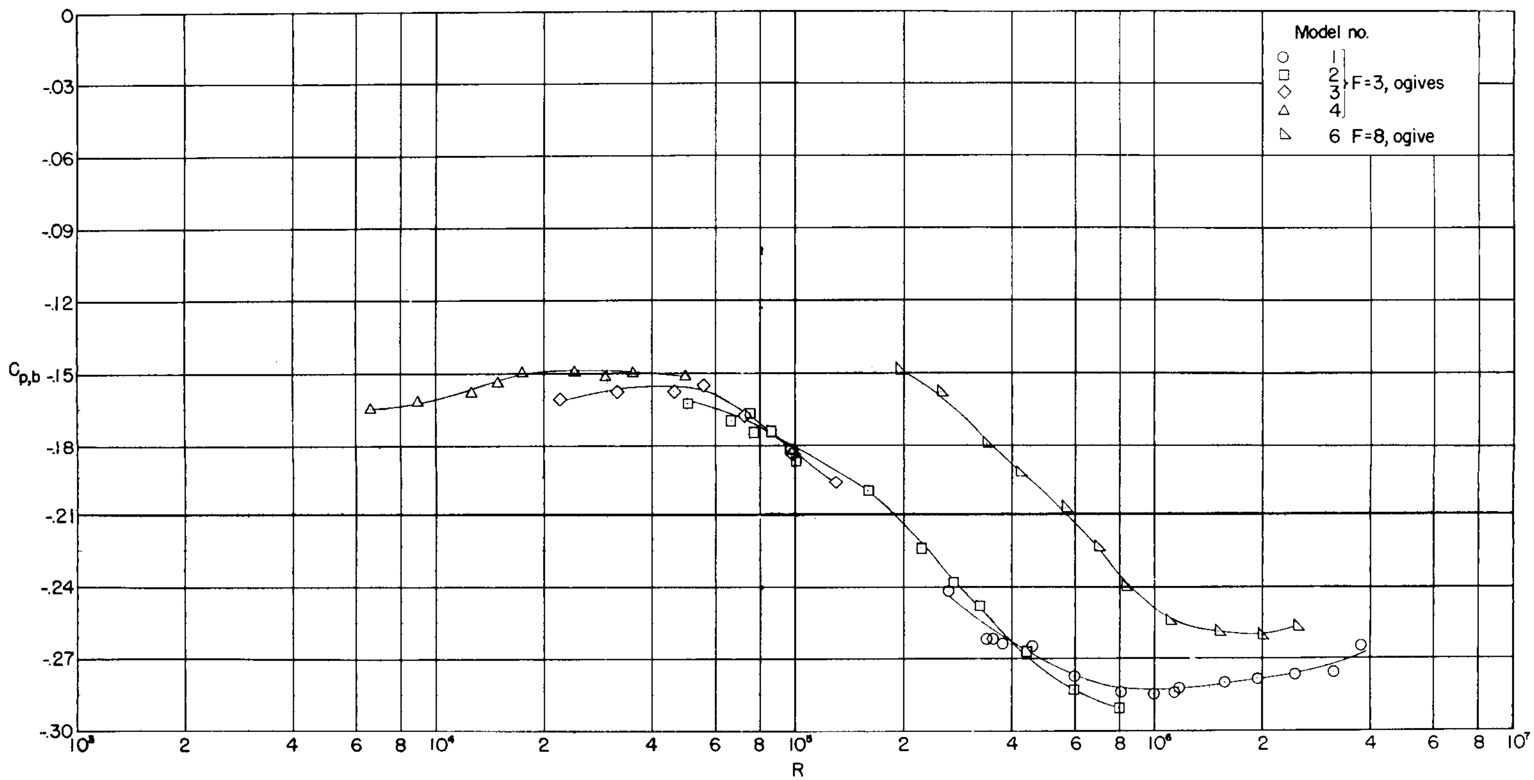

(a) $M_{nom} = 1.95$.

Figure 5.- Variation of base-pressure coefficient with Reynolds number.

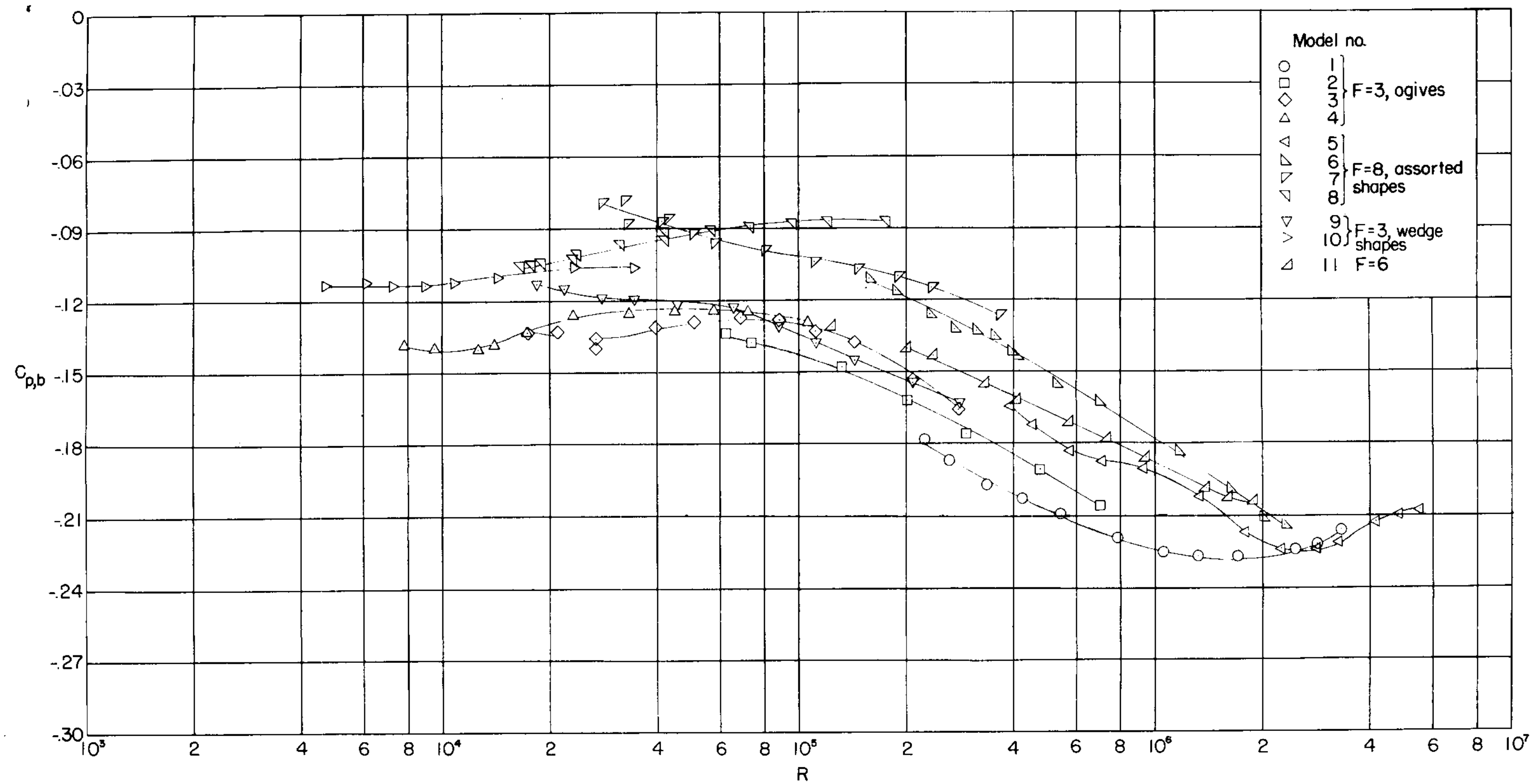

(b) M_{nom} = 2.22.

Figure 5.- Continued.

L-515

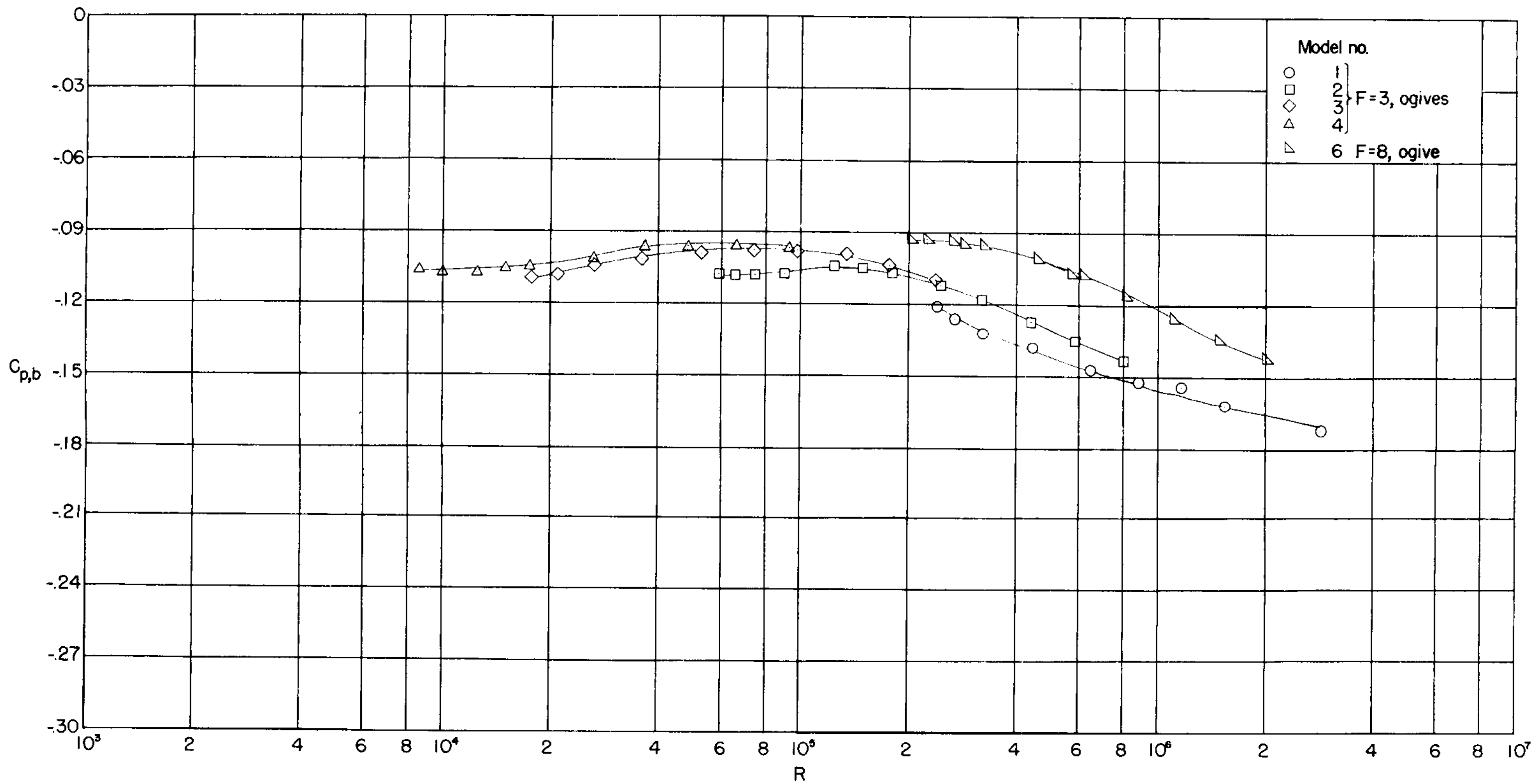

(c) $M_{nom} = 2.62$.

Figure 5.- Continued.

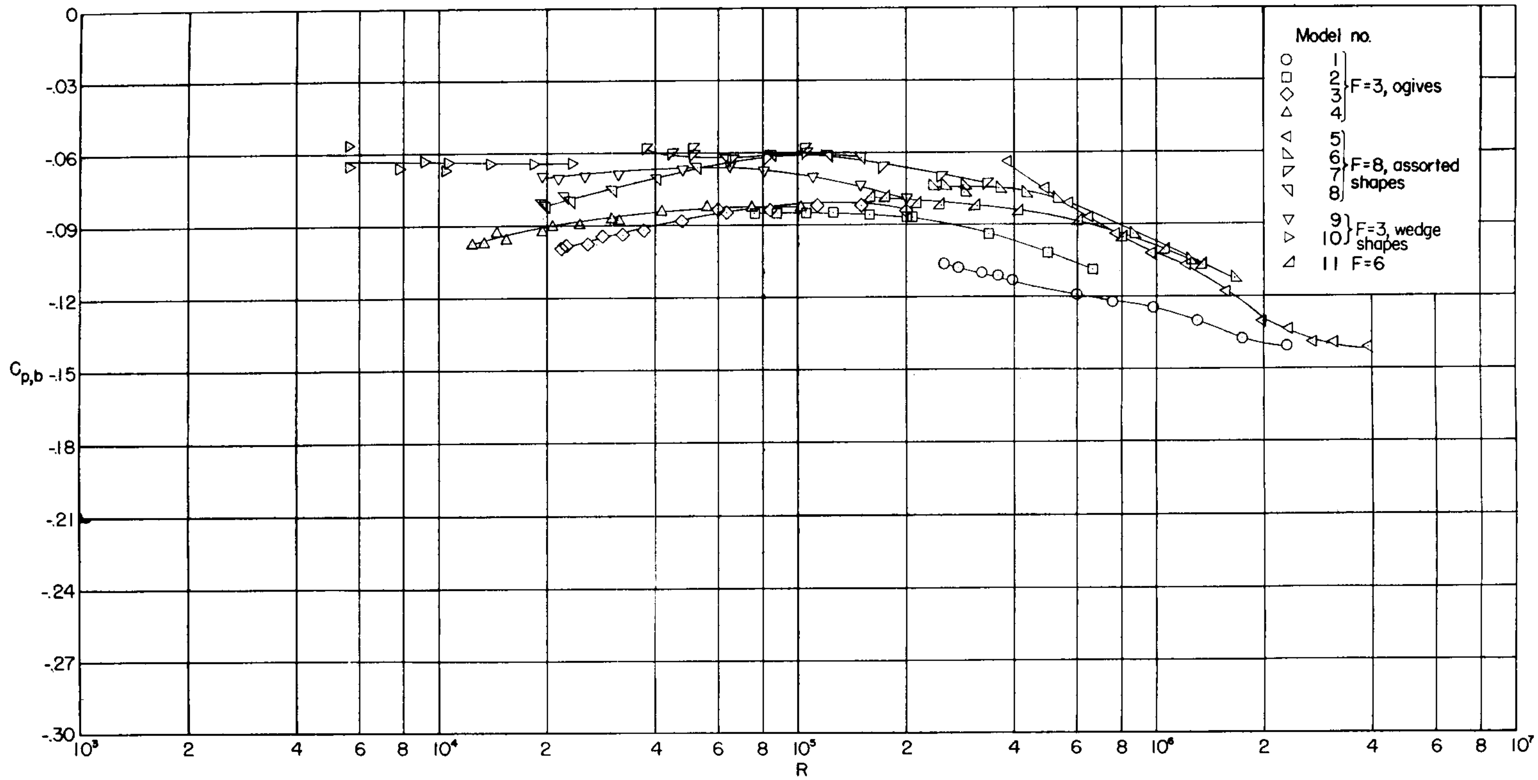

(d) $M_{nom} = 2.92$.

Figure 5.- Concluded.

L-515

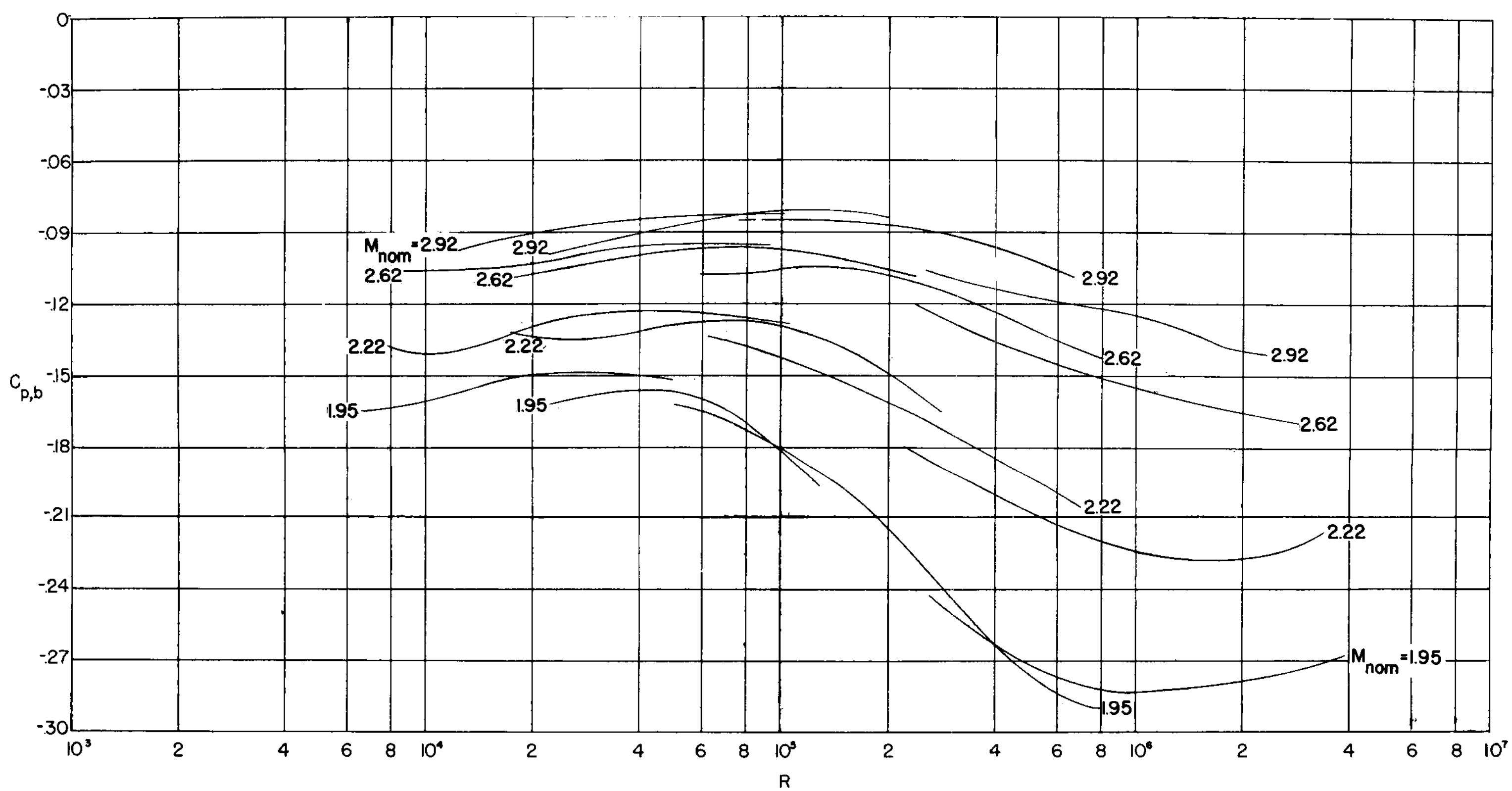

(a) F = 3, ogives.

Figure 6.- Variation of base-pressure coefficient with Reynolds number for models 1 to 8.

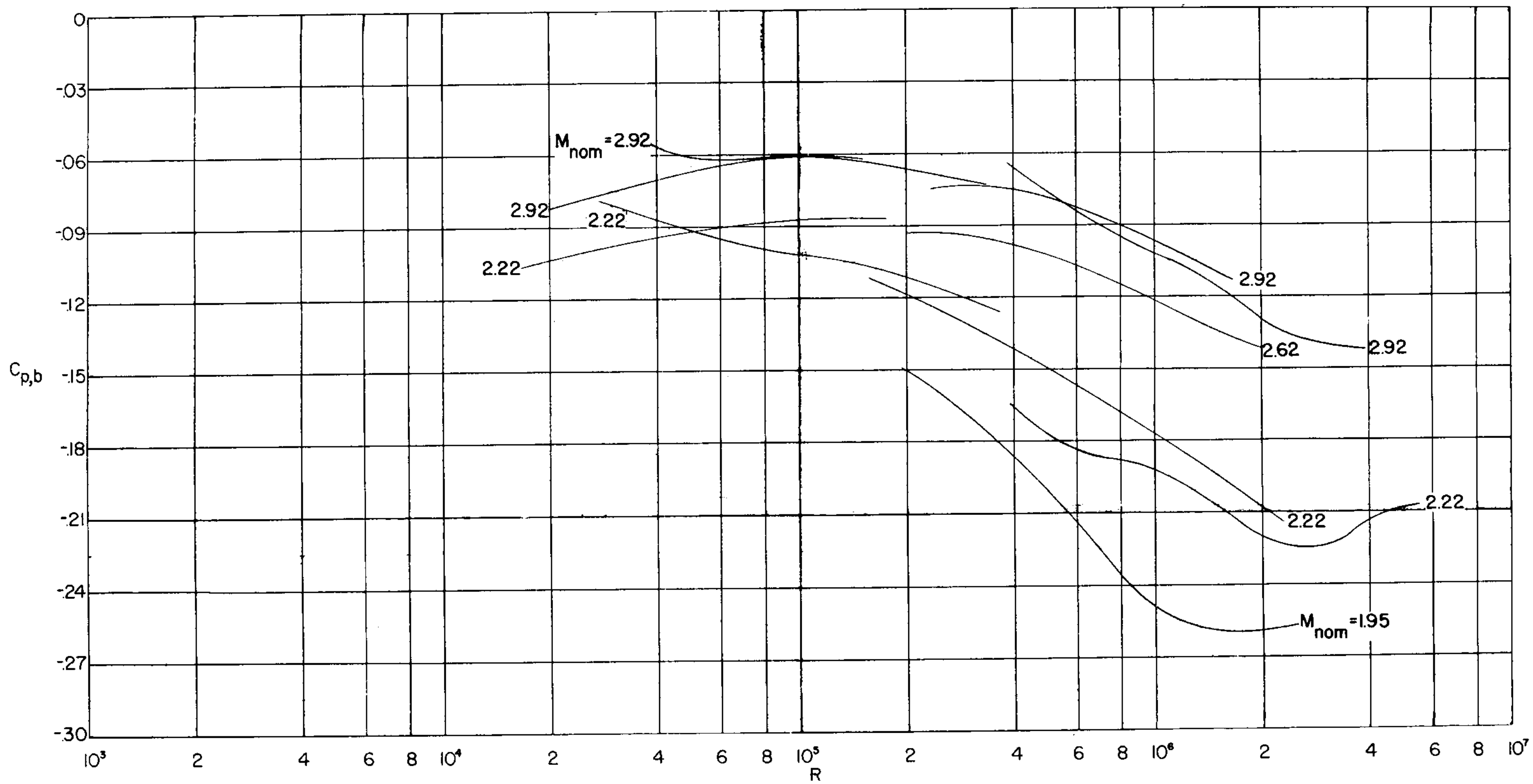

(b) F = 8, assorted shapes.

Figure 6.- Concluded.

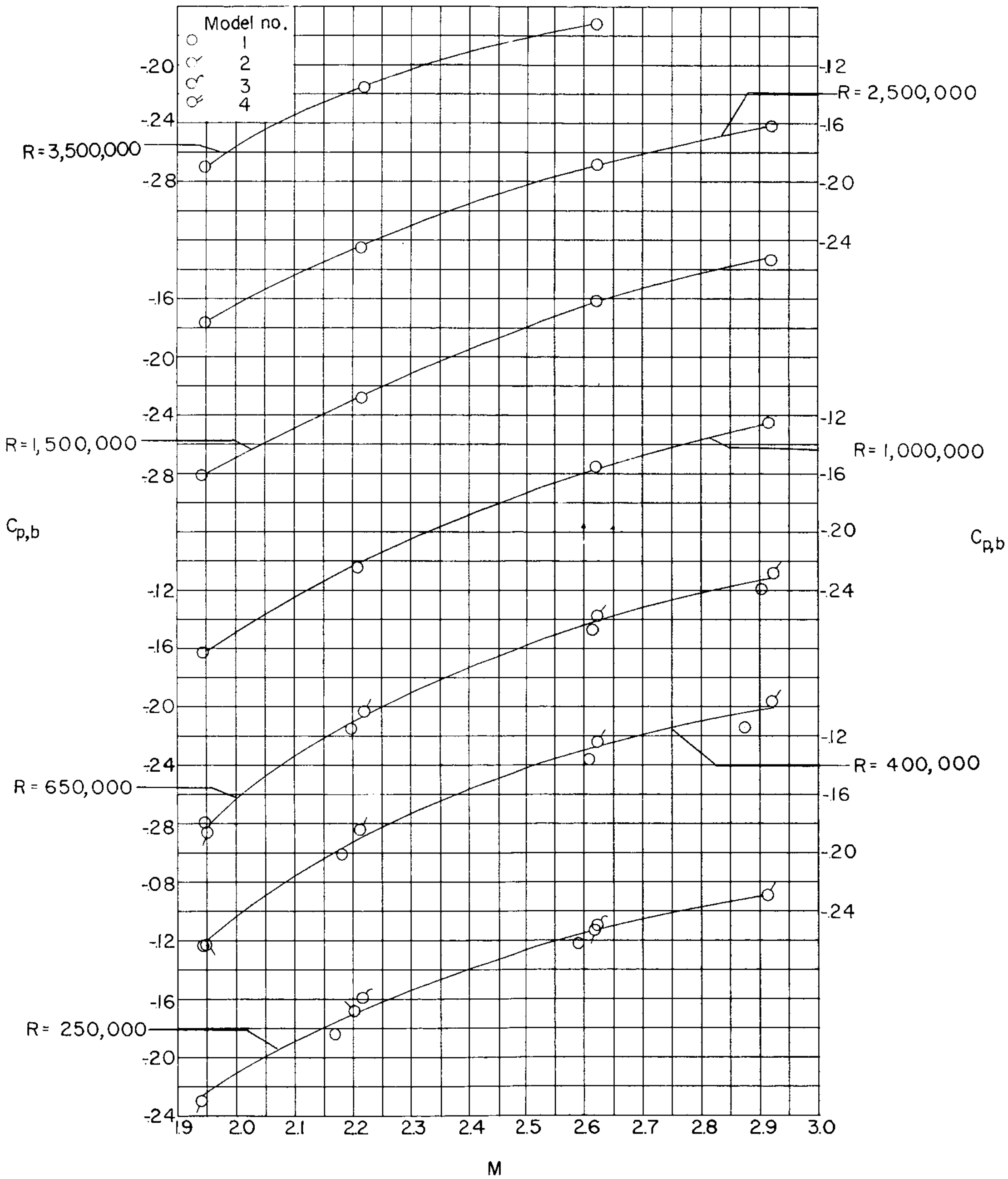

(a) F = 3, ogives.

Figure 7.- Variation of base-pressure coefficient with Mach number at constant Reynolds numbers.

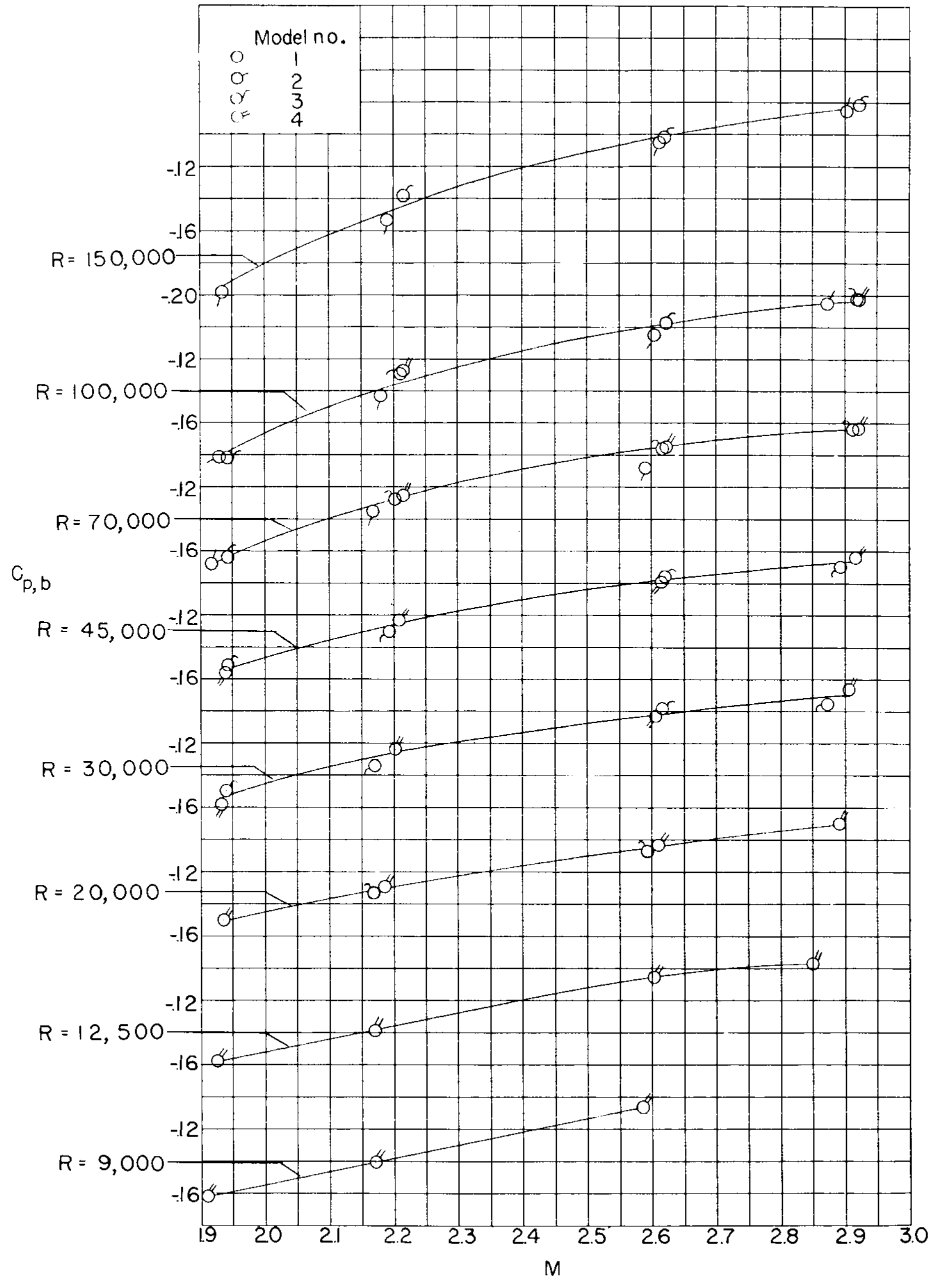

(a) Concluded.

Figure 7.- Continued.

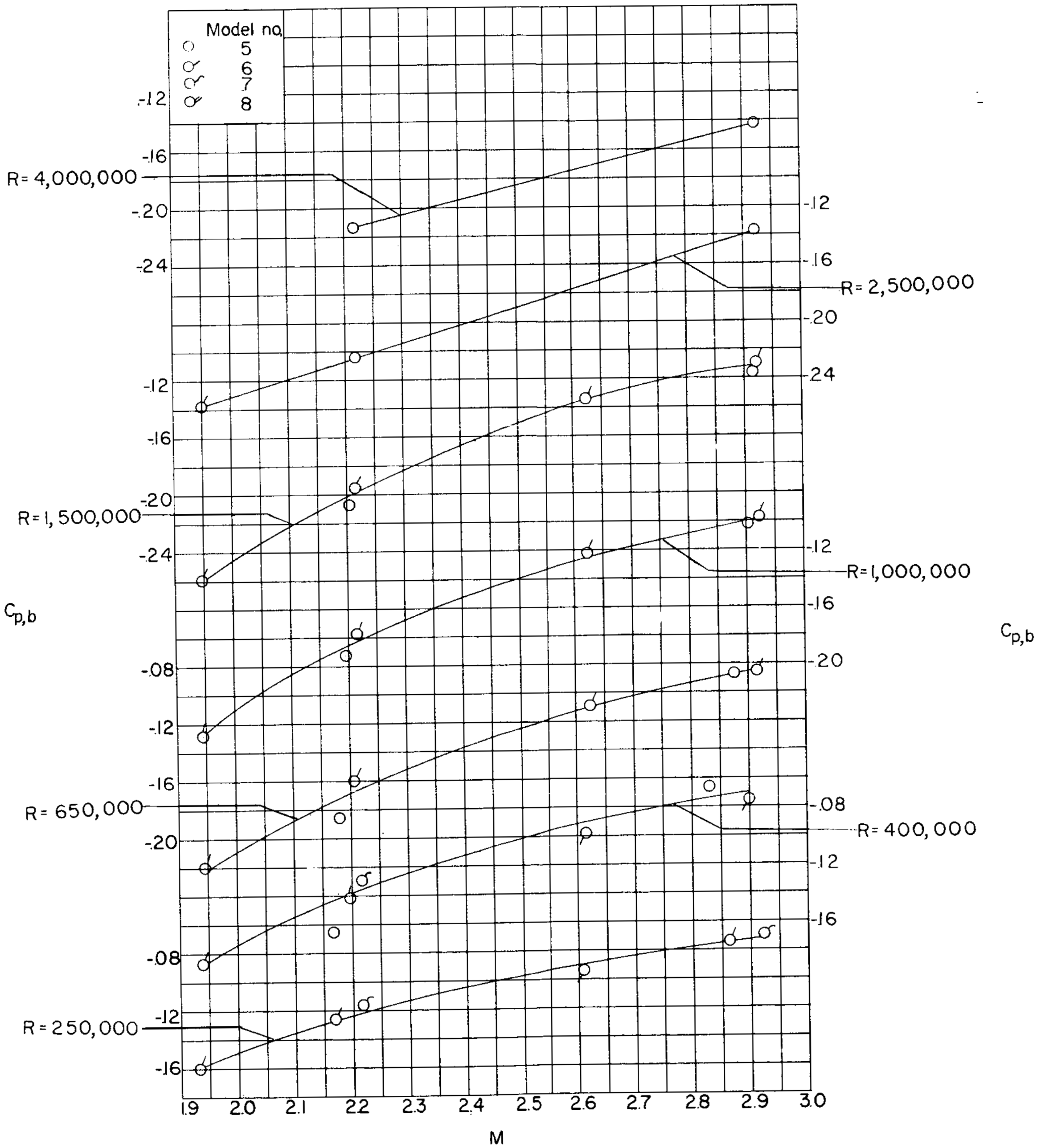

(b) F = 8, assorted shapes.

Figure 7.- Continued.

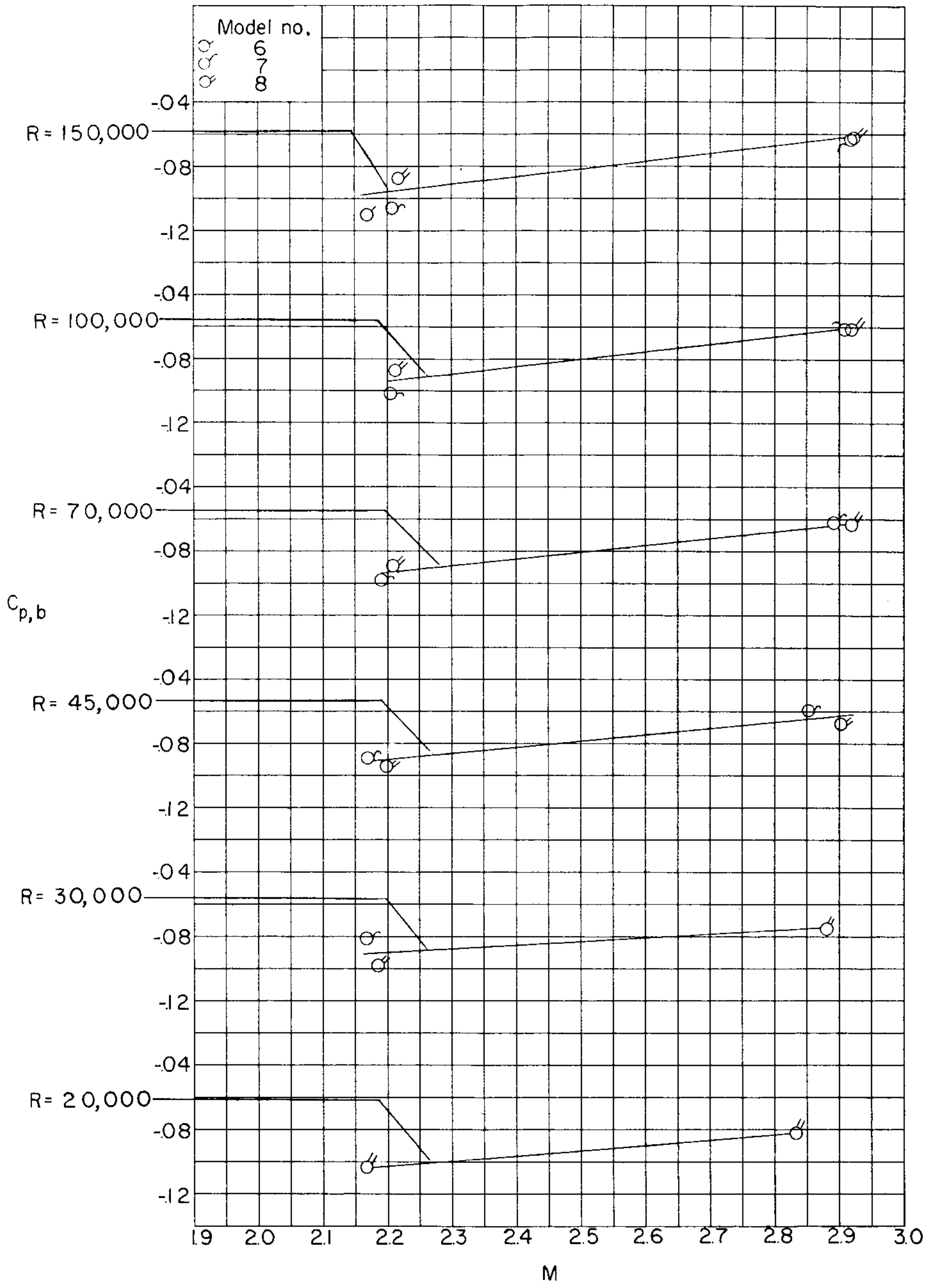

(b) Concluded.

Figure 7.- Concluded.

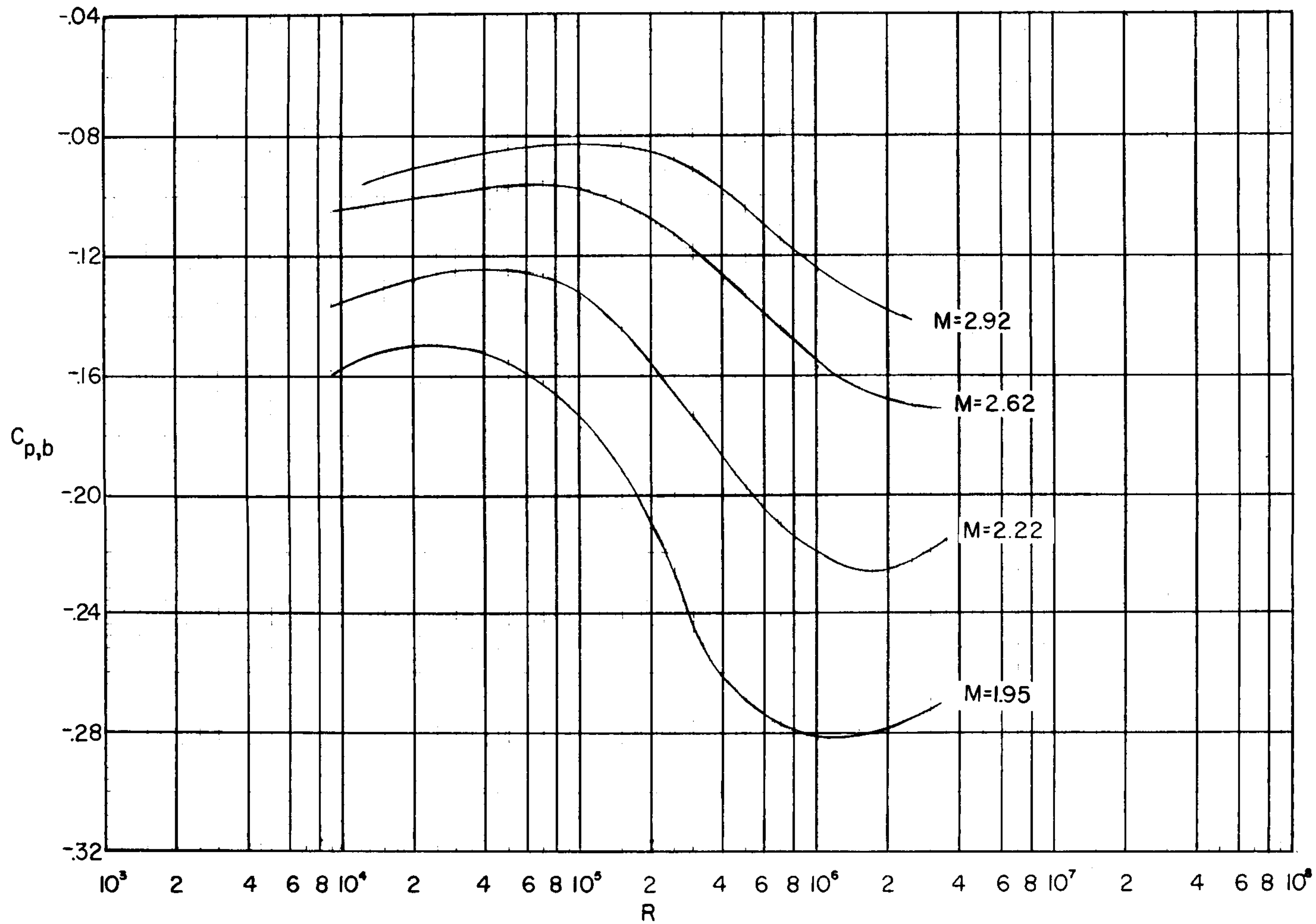

(a) F = 3, ogives.

Figure 8.- Final curves of variation of base-pressure coefficient with Reynolds number.

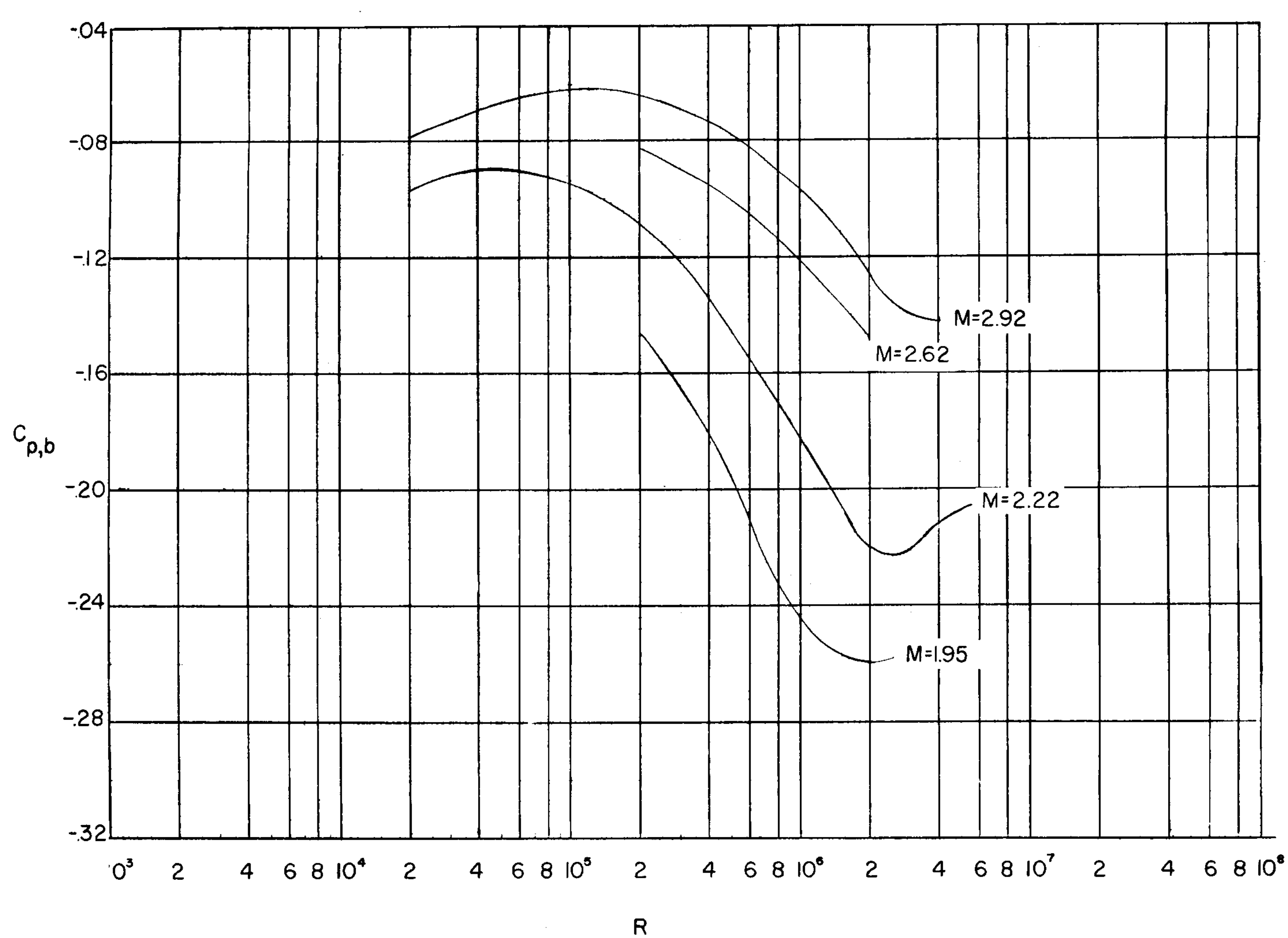

(b) F = 8.

Figure 8.- Concluded.

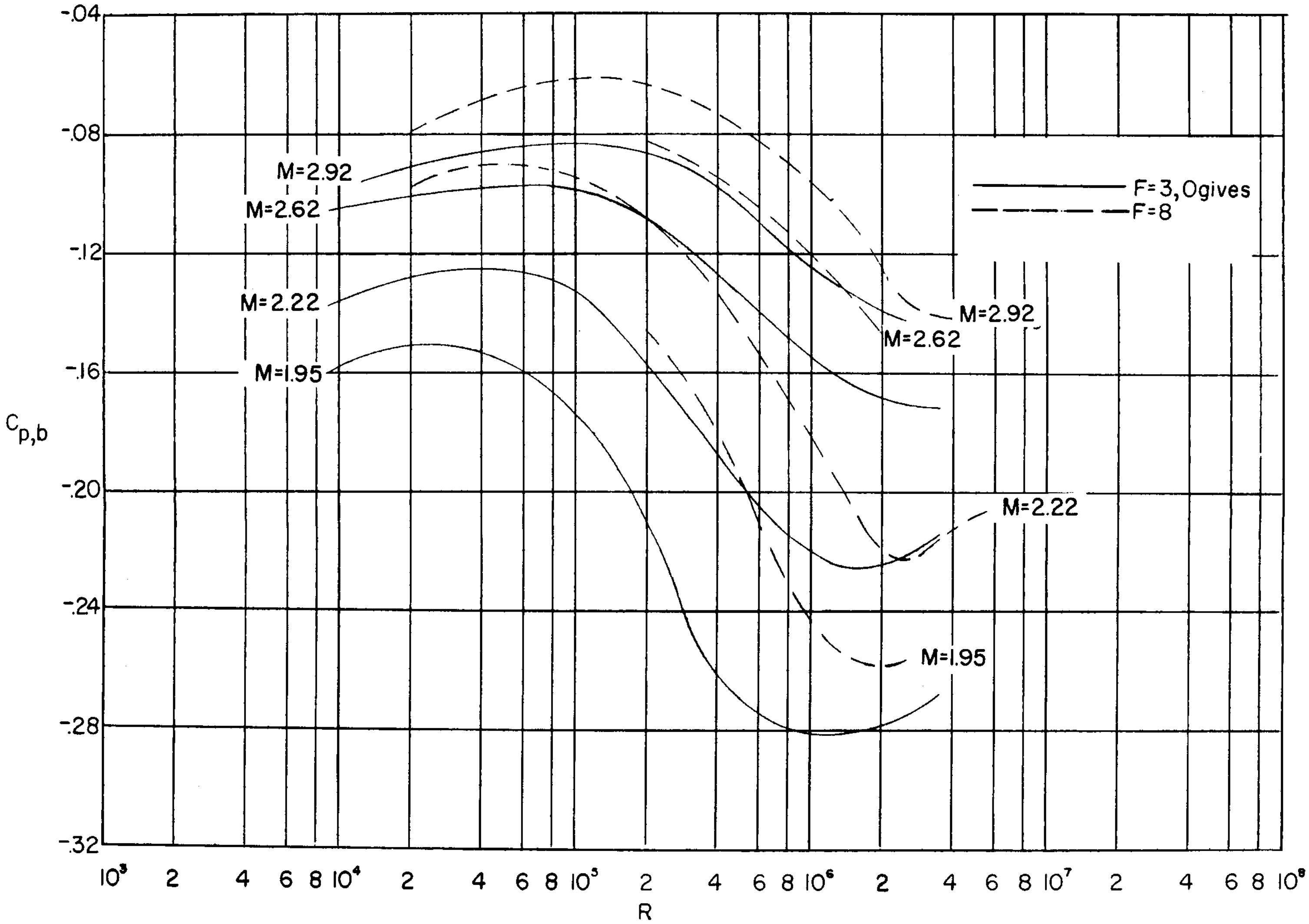

Figure 9.- Final curves showing fineness-ratio effect.

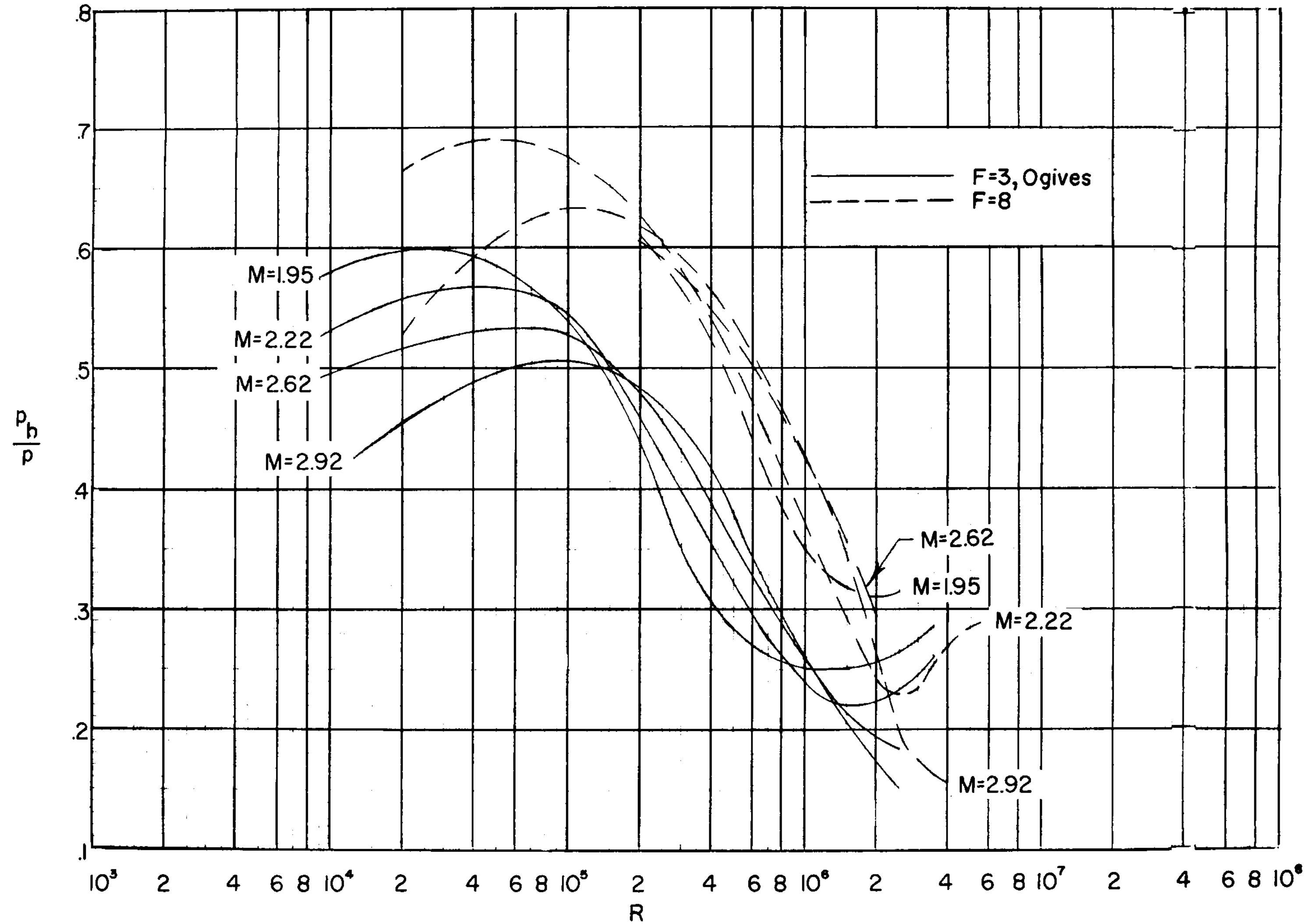

Figure 10.- Final curves of variation of base-pressure ratio with Reynolds number.

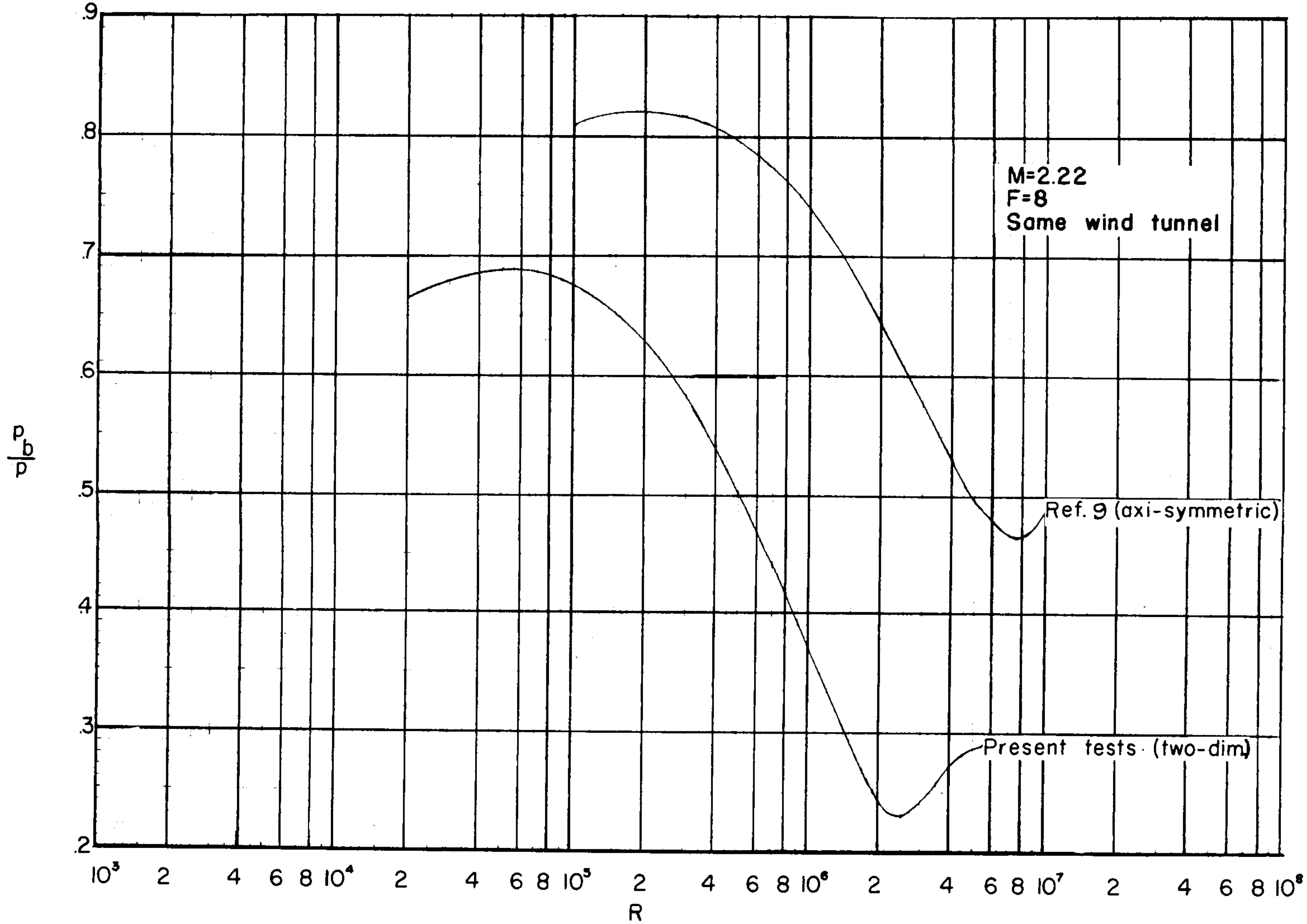

Figure 11.- Comparison between two-dimensional and axisymmetrical base pressure.

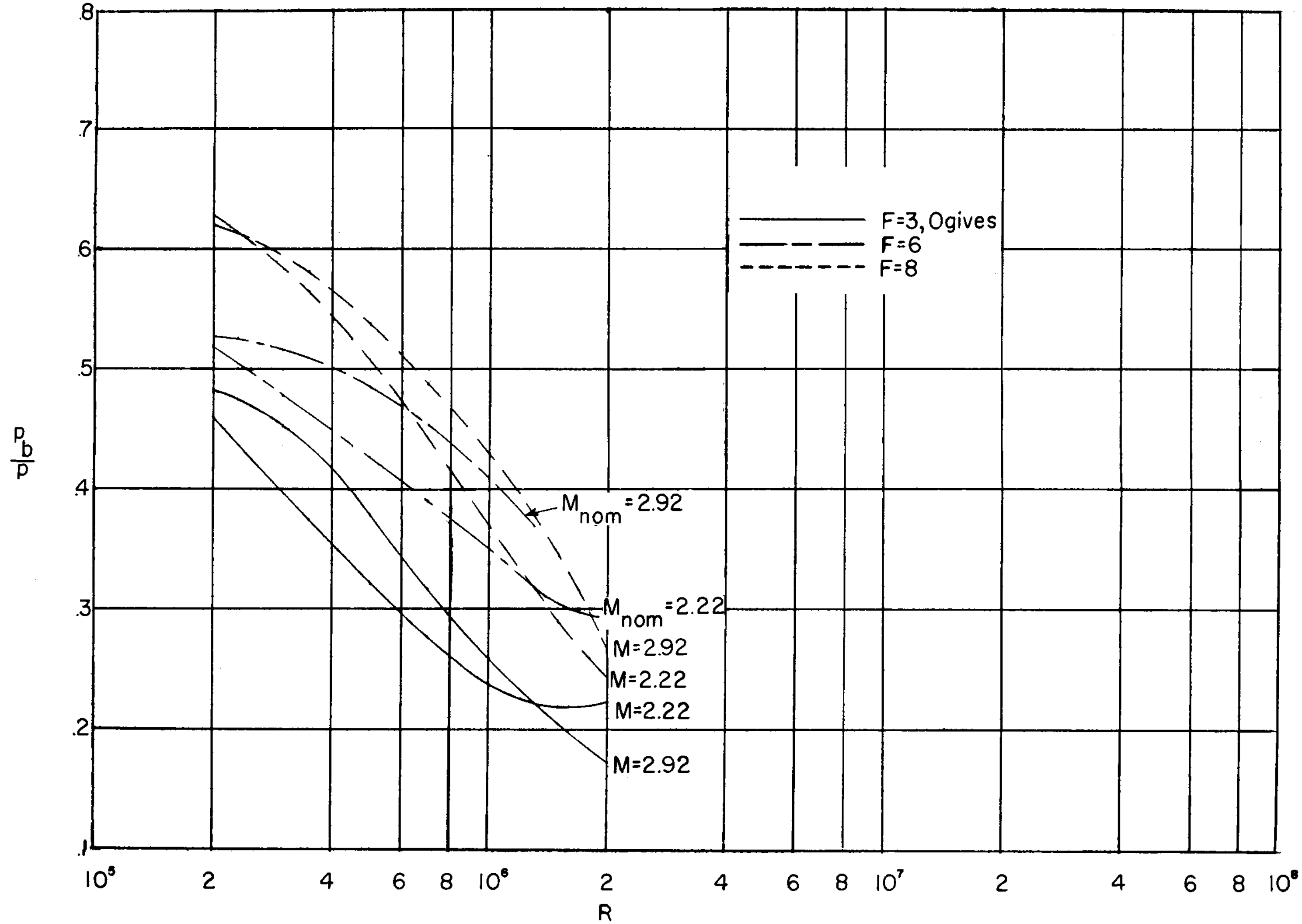

Figure 12.- Effect of fineness ratio upon base pressure.

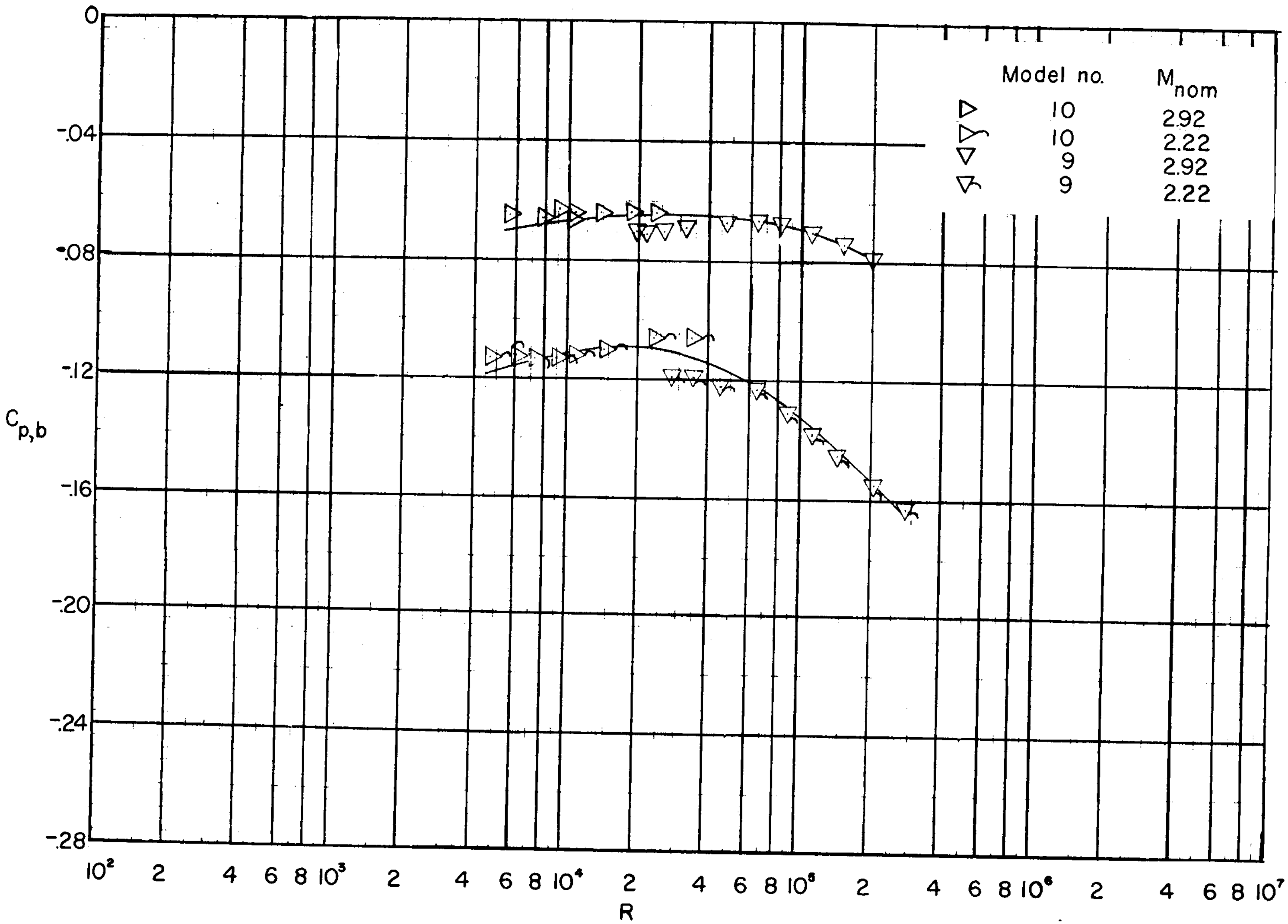

Figure 13.- Fairings of basic data for models 9 and 10 (F = 3; wedge, δ = 30°).

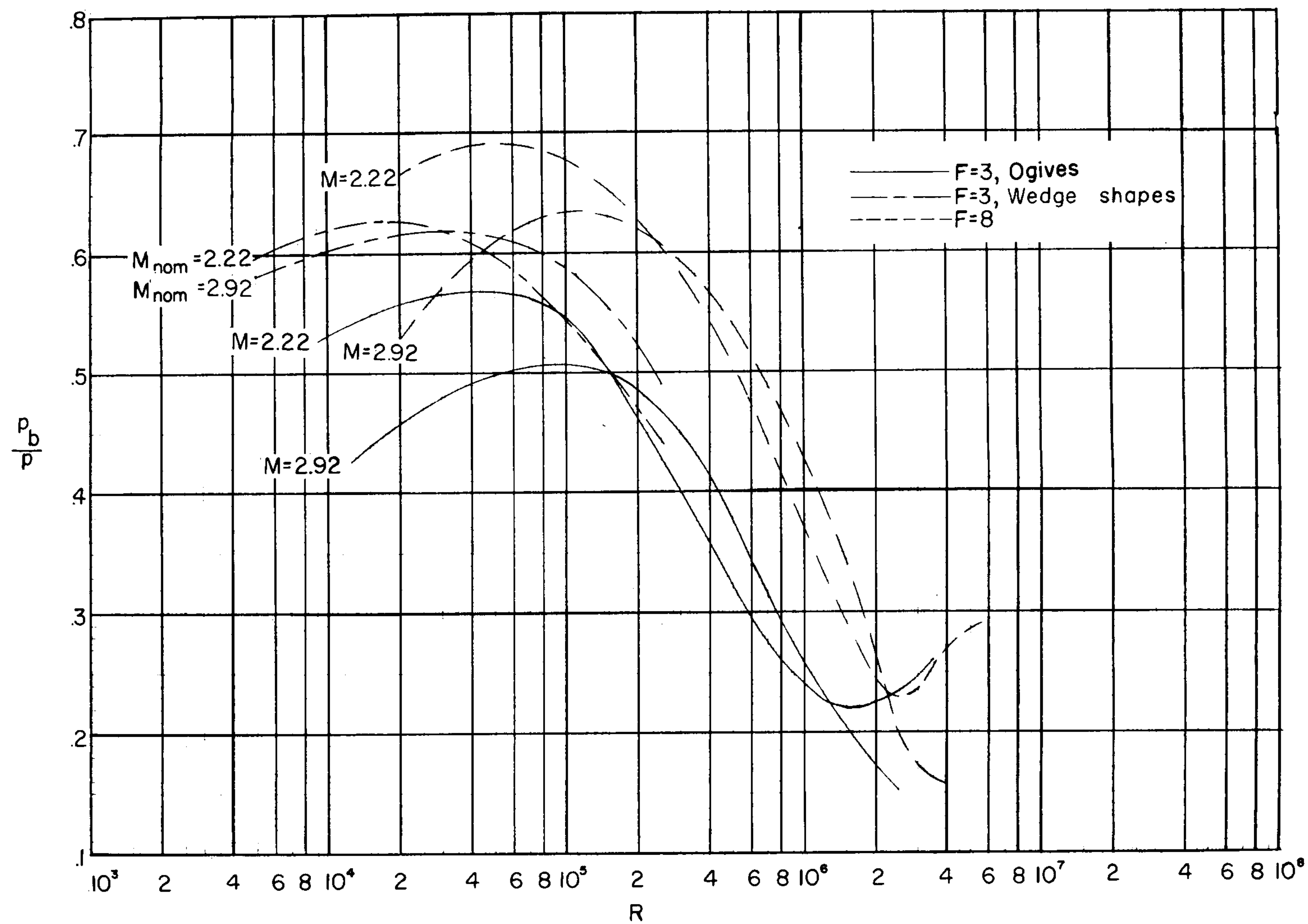

Figure 14.- Comparison of F = 3 wege shapes with other test shapes.

L-515

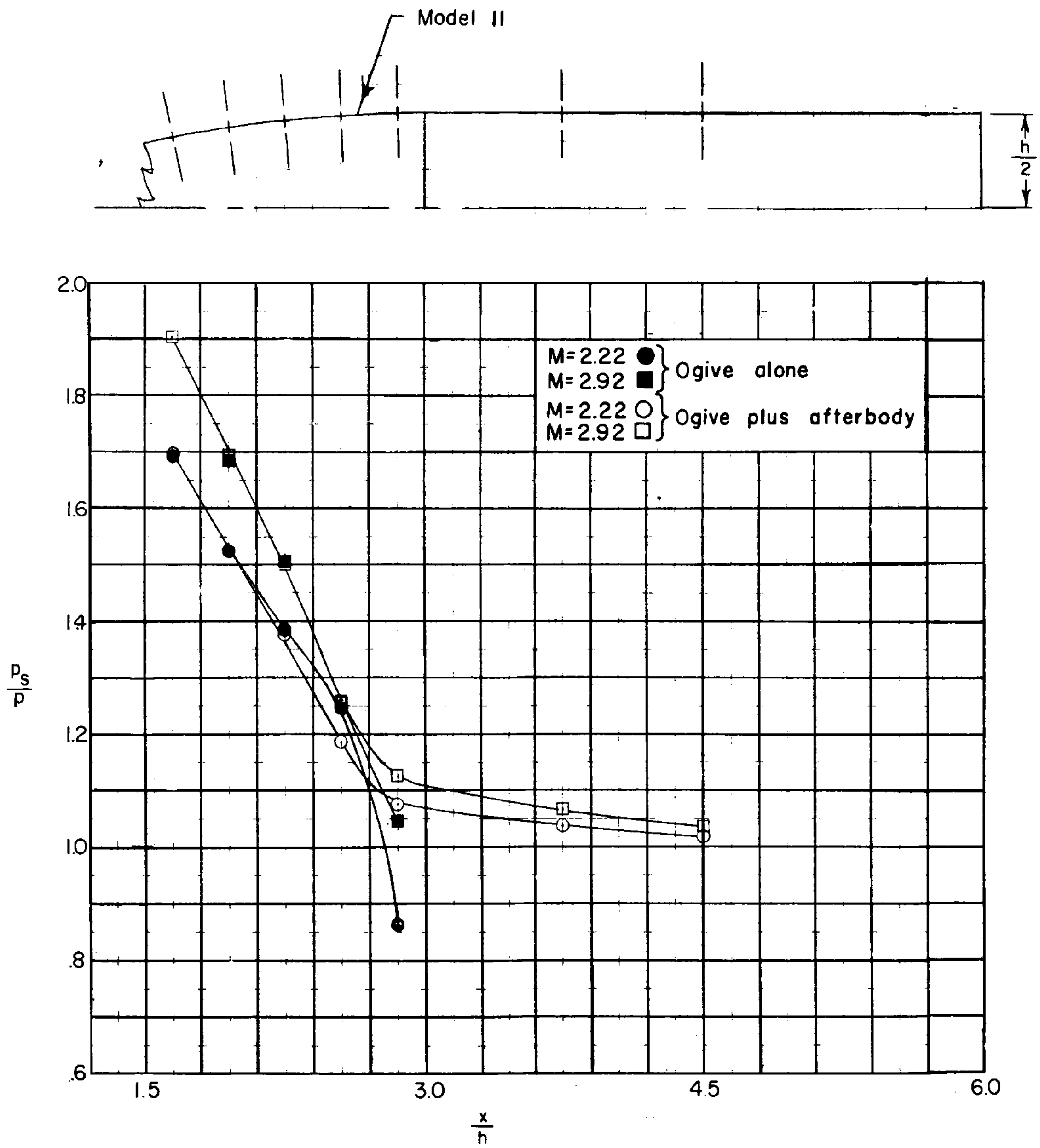

Figure 15.- Effect of base-pressure phenomena upon surface pressure (R = 300,000, based on chord length of ogive alone).

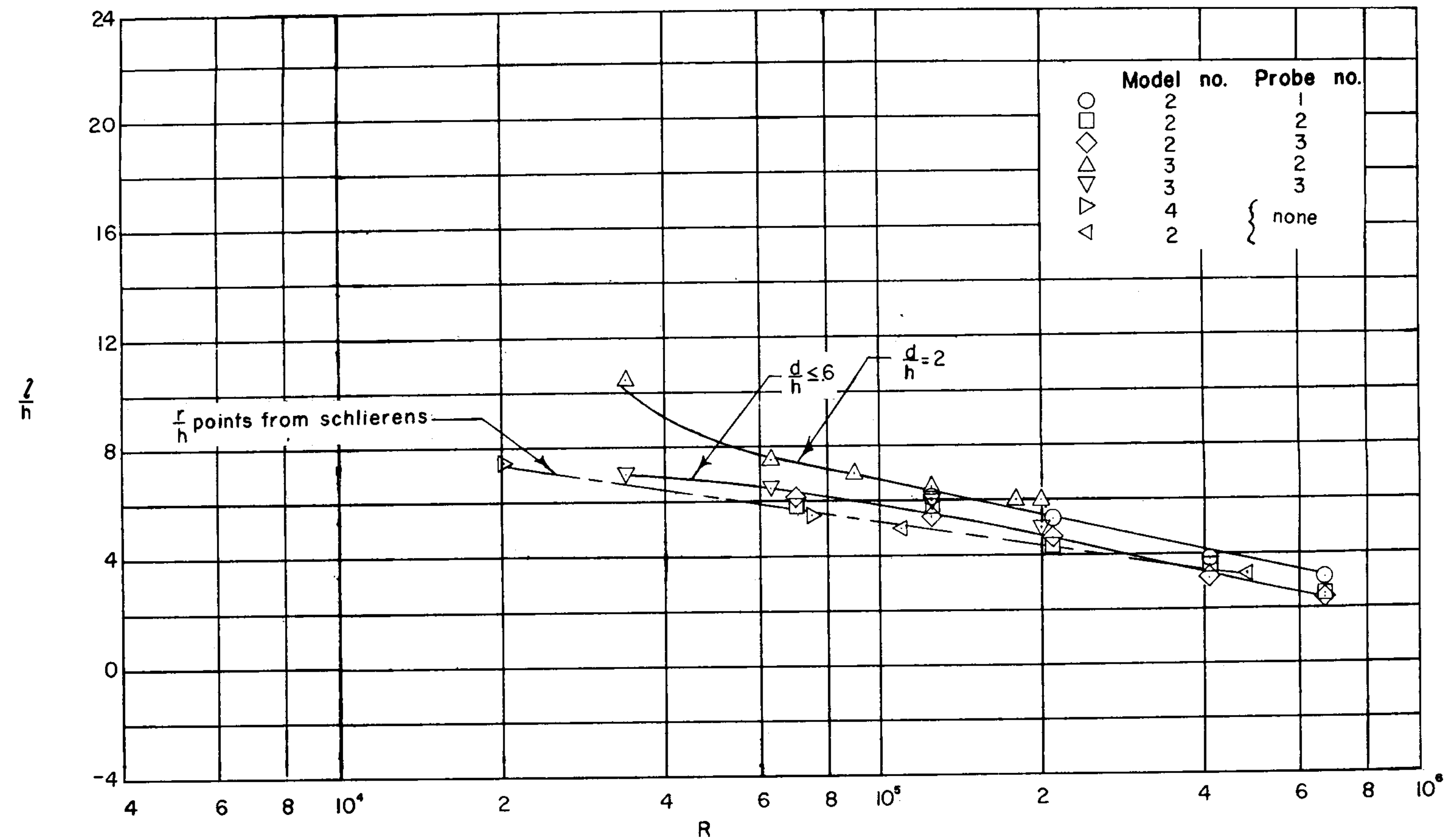

Figure 16.- Variation of minimum disturbance length (expressed in base heights) with Reynolds number at $M_{nom} = 2.92$.

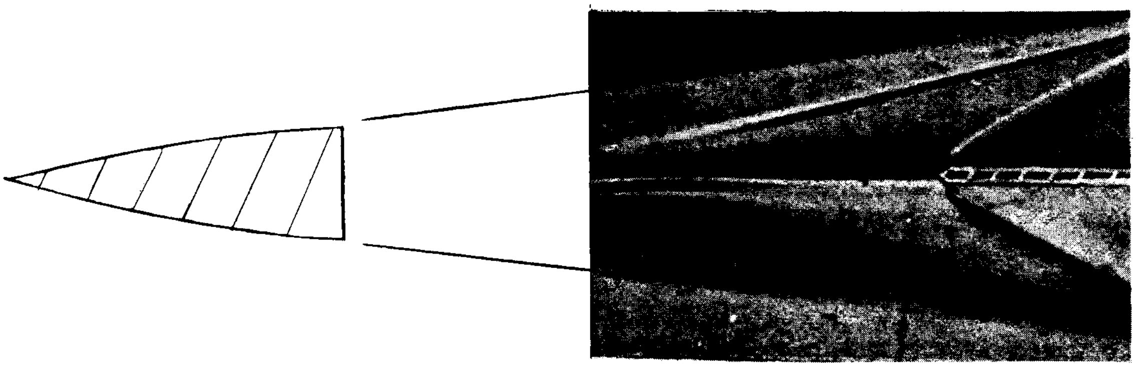

(a) $\frac{d}{h} = 0.09$; $\frac{l}{h} = 4.6$ (probe tip 5.4h from base).

L-715

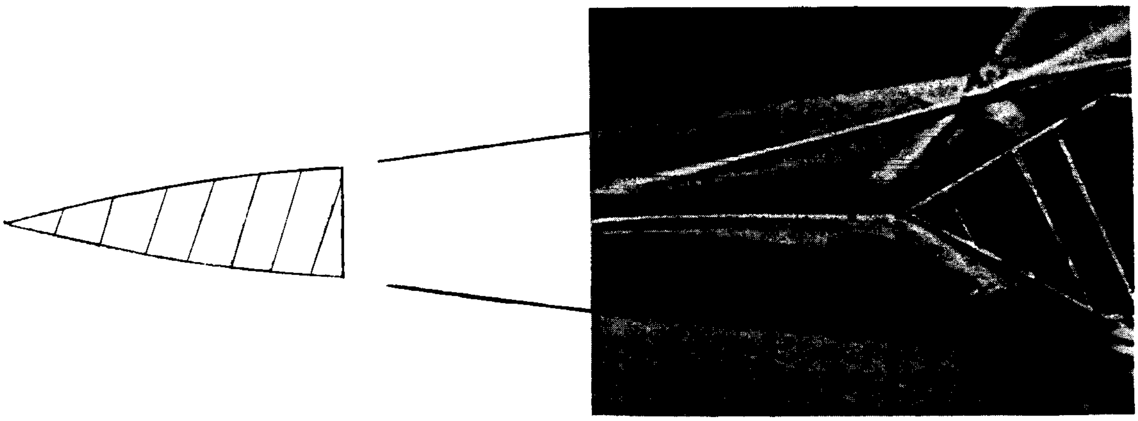

(b) $\frac{d}{h} = 2$; $\frac{l}{h} = 5.3$ (probe tip 5.3h from base).

L-59-6019

Figure 17.- Schlierens showing effect of disturbance probe height on l (model 2; R = 210,000; $M_{nom} = 2.92$).

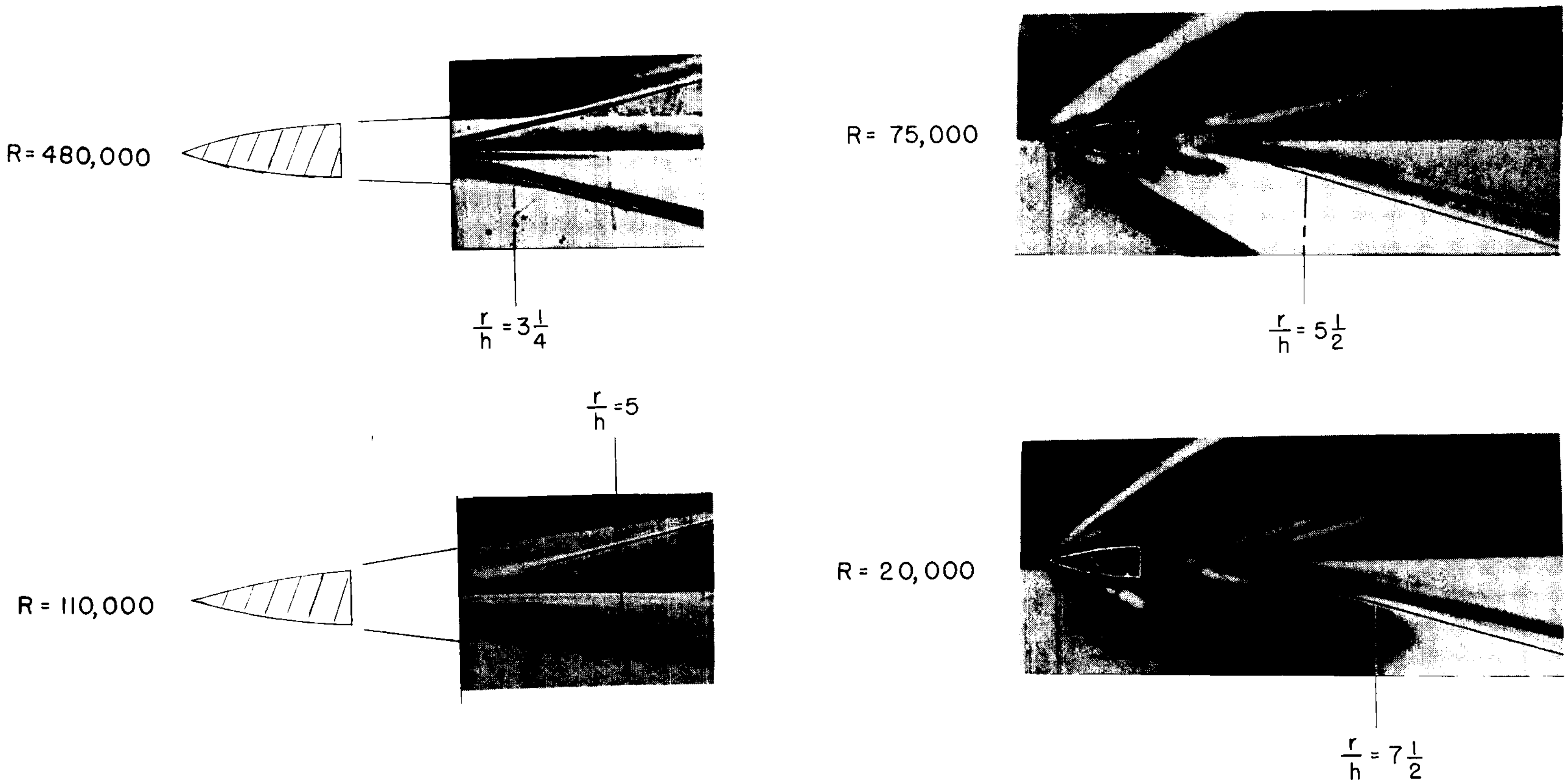

L-59-6020

(a) Model 2.

(b) Model 4 (wire supported).

Figure 18.- Schlieren study of variation of trailing-shock convergence point with Reynolds number at $M_{nom} = 2.92$.